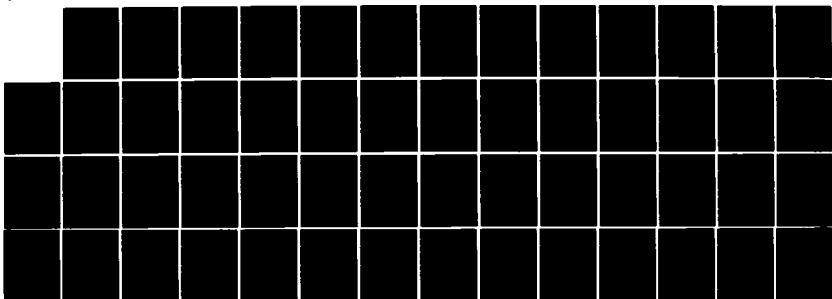
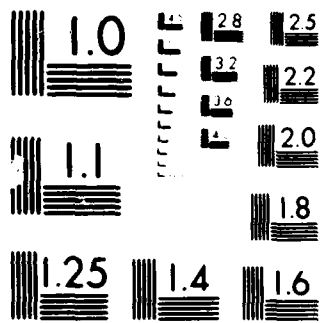


AD-A149 728 SCATHA (SPACERFRAFT CHARGING AT HIGH ALTITUDES) PLASMA 1/1
INTERACTION EXPERIM. (U) LOCKHEED MISSILES AND SPACE CO
INC PALO ALTO CA PALO ALTO RES. E G SHELLEY ET AL

UNCLASSIFIED 30 NOV 84 N00014-76-C-0444 F/G 22/2 NL





MICROSCOPY RESOLUTION TEST CHART
Nikon Microscope Resolution Test Chart

(12)

AD-A149 728

SCATHA FINAL REPORT
ONR Contract
N00014-76-C-0444

ONE FILE COPY

DTIC
ELECTRONIC
JAN 1 1985
S E D

 **Lockheed Missiles & Space Company, Inc.**
SUNNYVALE, CALIFORNIA

85 01 22 023

UNCLASSIFIED

SECURITY CLASSIFICATION OF THIS PAGE (When Data Entered)

12

REPORT DOCUMENTATION PAGE		READ INSTRUCTIONS BEFORE COMPLETING FORM
1. REPORT NUMBER	2. GOVT ACCESSION NO.	3. RECIPIENT'S CATALOG NUMBER
		1D-A149728
4. TITLE (and Subtitle) FINAL REPORT N00014-76-C-0444 SCATHA Plasma Interaction Experiment		5. TYPE OF REPORT & PERIOD COVERED Final Report for period 11-1-75 to 10-30-84
		6. PERFORMING ORG. REPORT NUMBER
7. AUTHOR(s) E. G. Shelley, R. D. Sharp, E. W. Nightingale, and J. M. Quinn		8. CONTRACT OR GRANT NUMBER(s) N00014-76-C-0444
9. PERFORMING ORGANIZATION NAME AND ADDRESS Space Sciences Laboratory, Dept 91-20, B255 Lockheed Palo Alto Research Laboratory 3251 Hanover Street, Palo Alto, CA 94304		10. PROGRAM ELEMENT, PROJECT, TASK AREA & WORK UNIT NUMBERS
11. CONTROLLING OFFICE NAME AND ADDRESS Mr. R. Gracen Joiner, Code 414 Office of Naval Research Arlington, VA 22217		12. REPORT DATE 30 November 1984
13. MONITORING AGENCY NAME & ADDRESS (if different from Controlling Office)		13. NUMBER OF PAGES 50 pp.
		14. SECURITY CLASS. (of this report) UNCLASSIFIED
		15a. DECLASSIFICATION/DOWNGRADING SCHEDULE
16. DISTRIBUTION STATEMENT (of this Report) Approved for public release; distribution unlimited.		
17. DISTRIBUTION STATEMENT (of the abstract entered in Block 20, if different from Report) Approved for public release; distribution unlimited.		
18. SUPPLEMENTARY NOTES		
19. KEY WORDS (Continue on reverse side if necessary and identify by block number)		
20. ABSTRACT (Continue on reverse side if necessary and identify by block number) <p>This report describes the results of the SC-3 (High Energy Particle Spectrometer) and SC-8 (Energetic Ion Composition Experiment) instruments flown on the SCATHA satellite, launched in January 1979 into a near geosynchronous orbit. The instruments measure electrons at energies of 0.05-5.0 MeV, protons of 1-100 MeV, and mass composition of ions in the range E/q=0.1-32. keV/e. Both instruments continue to be fully operational at this time.</p> <p>Principal results of the High Energy Particle Spectrometer have addres-</p>		

~~UNCLASSIFIED~~

SECURITY CLASSIFICATION OF THIS PAGE(When Data Entered)

20: sed radial profiles and energy spectra of energetic particles, the role of energetic particles in the charging and discharging of spacecraft dielectrics, the behavior of trapped electrons at flux levels near the Kennel-Petchek trapping limit, and the precipitation of energetic electrons into the ionosphere.

The Energetic Ion Composition Experiment has provided the first ion composition data with routine pitch angle coverage in the vicinity of geo-synchronous orbit. The advances resulting from this instrument can be grouped into four categories: (1) plasma injection and transport, (2) detailed structure of near-geosynchronous plasma distributions, (3) interactions between hot plasmas and spacecraft, and (4) global understanding arising from the synthesis of individual results.

Accession For	
NTIS GRA&I	<input checked="" type="checkbox"/>
DTIC TAB	<input type="checkbox"/>
Unannounced	<input type="checkbox"/>
Justification	
By _____	
Distribution/ _____	
Availability Codes	
Avail and/or	
Dist	Special
A-1	



~~UNCLASSIFIED~~

SECURITY CLASSIFICATION OF THIS PAGE(When Data Entered)

Final Report

Preliminary Approval Copy

ONR Contract N00014-76-C-0444

SCATHA Plasma Interaction Experiment:

SC-3 High Energy Particle Spectrometer

SC-8 Energetic Ion Composition Experiment

November 30, 1984

INTRODUCTION

The High Energy Particle Spectrometer (SC-3) and Energetic Ion Composition Experiment (SC-8) were launched in January 1979 aboard the P78-2 spacecraft as part of the Spacecraft Charging AT High Altitudes (SCATHA) payload. The SCATHA instrument complement was designed to study spacecraft responses to the ambient environment, particularly the electrical charging and discharging processes arising from natural particle fluxes and from the operation of onboard electron and ion guns. Instrumentation included sensors of the particle, field, and wave environment; monitors of transient pulses, surface potential and contamination; and electron and ions guns designed to actively control the spacecraft potential with respect to the surrounding plasma. Descriptions of the instruments have been compiled by Stevens and Vampola (1978).

The SC-3 high energy particle spectrometer uses a stacked set of four solid state sensors. Programmable logic combinations of the four sensors are used to select various particle types and energy ranges on a time multiplexed basis and to discriminate against unwanted background. Outputs from a twelve channel pulse height analyzer, set to the desired energy range, are accumulated in 0.5 second periods. The detector normally senses electrons from 0.05-5.0 MeV and is capable of measuring protons from 1-100 MeV and alpha particles from 6-60 MeV. The three degree field of view is oriented perpendicular to the spacecraft spin axis, providing good pitch angle coverage. Details of the SC-3 instrument are given in Appendix 1, which has been excerpted from Stevens and Vampola (1978).

The SC-8 energetic ion composition experiment has 3 detector heads, each using a crossed electric and magnetic field velocity filter in combination with an electrostatic analyzer to select ions of the desired mass/charge. Ion fluxes are measured in 24 energy channels covering $E/Q=0.1-32$. keV/e. The instrument's

normal mass range of 0.8-80 AMU is covered in 30 steps. In addition, fixed magnetic analyzers measure electrons in four broad bands from 0.07 to 24 keV. SC-8 is oriented 79 degrees from the spacecraft spin axis, and routinely obtains good coverage of fluxes closely aligned with the magnetic field. Details of the SC-8 instrument are given in Appendix 2 which has been excerpted from Stevens and Vampola (1978).

The performance of the SC-3 and SC-8 instruments has been excellent, and the instruments are continuing to acquire data at this time. Digitized data tapes are available for all days from launch through early 1980, as well as for many later periods.

The following sections of the report summarize the principal scientific results which have been obtained to date. The three appendices describe the SC-3 and SC-8 instruments and provide abstracts of all publications.

RESULTS OF THE HIGH ENERGY PARTICLE EXPERIMENT

The energetic electron intensities measured by SC-3, with its fine-resolution energy spectra and pitch-angle distributions, have been used to further our knowledge of the radiation environment in the near-geosynchronous region, spacecraft charging, and wave-particle interactions that enhance particle precipitation.

The radial profiles and energy spectra as determined from SC-3 during the SCATHA transfer orbit have been compared to the NASA AE-4 and AEI-7 HI/LO radiation models of the outer belts (Reagan et al., 1981a). Agreement with the AE-4 model was good up to the 4 MeV limit of the model.

The SC-3 data have been used to investigate the role that energetic particles in the substorm plasma have on the charging and discharging of typical

dielectric layers used on spacecraft (Reagan et al., 1981b). The spectra and pitch-angle distributions of electrons and protons were used to study the time periods prior to, and during, a few-kilovolt differential charging event initiated by a substorm while the SCATHA spacecraft was in the eclipse condition on March 28, 1979. The data used in the analysis included lower-energy electron and proton measurements from the Lockheed SC-8 ion composition experiment. The charging current density carried by the higher-energy electrons was found to be within a factor of 5 of the maximum allowable trapping limit according to experimental verifications of the Kennel-Petschek theory.

During the period of June 11 to 14, 1980, fluxes of high energy electrons (1 to 5 MeV) were greatly intensified in the near-geosynchronous region following a magnetic storm (Gaines et al. 1981). The flux on June 14 has been the hardest yet seen by SC-3. It was concluded that damage due to short-term effects, such as charging and possible rapid discharging in dielectrics from the accumulation of electrons stopped in the material in a period of the order of a day, was more likely than total dose damage over the few days duration of high, hard flux levels.

The range and limits on the space charging electron currents available in the near-geosynchronous orbit were identified from a large SC-3 data base (Reagan et al., 1983). The most intense current densities observed were 0.8 nA/cm^2 at 1 keV and 0.5 pA/cm^2 at 1 MeV. These establish an upper limit to which spacecraft need to be tested in order to withstand space charging currents. The effects of these currents on both surface and internal charging of dielectrics have been modeled. The electric field strengths were near minimum breakdown level, but the transient pulses observed on SCATHA may be associated with the internal redistribution of these fields. This can occur at the times of large and rapid flux changes or at the times that heavy cosmic-ray tracks locally discharge the highly charged dielectrics.

In studying the behavior of trapped electrons near the Kennel-Petschek trapping limit, the SC-3 energetic electron data have been utilized to demonstrate and confirm that the energy-dependent flux limit is very sensitive to the electron flux anisotropy and to the plasma conditions (Davidson et al., 1984). In every one of 12 cases selected from the SC-3 data for analysis in this study, a limited energy range was found where flux limiting appeared to be acting. This included moderately quiet times, when the flux limiting region was typically from tens of keV to several hundred keV; high flux events, when the limiting region was from \geq 50 keV to several hundred keV; and hard-spectrum cases, where flux limiting appeared to be acting from several hundred keV to beyond 1 MeV. The increases in the energetic electron flux and the build-up of the low energy plasma followed by short periods of filled loss cones provides direct evidence for strong diffusion in the radiation belts.

A study of three coordinated observations of precipitating energetic electrons during moderate to active times ($K_p = 3$ to 6) using the near-geosynchronous SCATHA spacecraft and the low altitude (~600 km), polar orbiting P78-1 satellite was carried out (Filbert et al., 1984). The Lockheed instrument package on P78-1 included two energetic electron detectors at high and low sensitivity over the energy range of ~60 keV to 1.2 MeV. Comparisons of the temporal flux profiles, energy spectra and pitch-angle distributions for electrons measured by P78-1 and SC-3 on SCATHA were made near the magnetic and temporal conjugacy as determined by the Olsen-Pfizer geomagnetic field model. In two of the cases studied the same flux level, spectral shape and e-folding energy for the two satellite data sets were obtained within 5% of the L-shell predicted by the model, even though there was moderate to intense geomagnetic activity. Some differences appeared in the third case. All three cases showed flux limiting over some portion of the energy range.

Satellite bremsstrahlung x-ray measurements on the P78-1 spacecraft have been compared to direct electron (>68 keV) measurements on board P78-1 (Imhof et al., 1982b) and to coordinated electron (47-66 keV) measurements from the SC-3 SCATHA experiment (Imhof et al., 1982a), as well as from balloon and riometer measurements. The remote sensing of precipitating energetic electrons by the measurement of bremsstrahlung x rays over much larger spatial regions than provided by the in situ observations of the electrons at the spacecraft provides new insight into the understanding of the detailed temporal occurrences of electron precipitation during magnetosperic substorms.

Over 8 months of spin-averaged SC-3 energetic electron fluxes have been processed into a computer data base, ready for further analysis. This data base has been the starting point for several of the above studies and should continue to be useful in further studies of the dynamic outer radiation belt region, spacecraft charging and wave-particle interactions that enhance particle precipitation.

RESULTS OF THE ENERGETIC ION COMPOSITION EXPERIMENT

The SC-8 instrument provided the first ion composition data with routine pitch angle coverage in the region near geosynchronous orbit. The 5 degree FWHM pitch angle resolution has allowed exploration of many of the highly anisotropic particle populations which are observed in this region of space. In addition, SC-8 extended the range of hot plasma composition measurements upward by a factor of two, to 32 keV/e.

Analyses of this unique data set have addressed a wide range of problems, ranging from specific particle energization processes to spacecraft-environment interactions to global magnetospheric plasma circulation. The results of these

studies may be broadly grouped into four categories: 1) Plasma injection and transport, 2) Detailed structure of plasma distributions, 3) The hot plasma environment and spacecraft interactions, and 4) Global synthesis of ion composition results. The contributions in each of these areas are summarized below.

Plasma Injection and Transport

One fundamental contribution of ion composition data is the ability to differentiate plasmas of different sources (ultimately of solar wind or ionospheric origin) by measuring the relative abundances of certain characteristic species. This ability is crucial in understanding the transport, energization, and loss histories of various plasma components. It has long been known that at the time of magnetospheric substorms, fresh energetic plasma is observed in the vicinity of geosynchronous orbit. This plasma is "injected" by some combination of ionospheric upflow, local energization, and inward transport from the plasma sheet. The capability to differentiate ion species has been exploited within the SC-8 data to investigate the processes by which plasma injection into the magnetospheric population occurs.

The dispersion of substorm injected ions was analyzed for species and pitch angle variations in two events for which SCATHA was moving through the noon to dusk local time sector (Strangeway and Johnson, 1983a). A clear dispersion ridge was observed for both H^+ and O^+ . At low pitch angles, H^+ ions were found to arrive at the spacecraft consistently ahead of O^+ . Prior to each of the dispersion events, it was noted that both species were greatly depleted in the dayside magnetosphere. The dispersion features were proposed to be primarily the result of direct ionospheric injection, with more energetic protons coming from the plasma sheet.

Another ion dispersion event was analyzed and compared with predictions of the injection boundary model, in which plasma is assumed to be injected in the region tailward of a spiral shaped boundary in the nightside magnetosphere (Strangeway and Johnson, 1983b). It was concluded that the injection boundary indeed provides a fairly good representation of the inner limit of ion injection.

A class of particularly intense field-aligned ions were observed to occur in association with some of the substorm ion injection events (Quinn and Johnson, 1984). These ions have a much narrower energy-time dispersion signature than the previously described events, and thus correspond to a very limited source region. Detailed comparison of this narrow signature with model dispersions and with plasma data from the UCSD SC-9 instrument show that the ions have a particularly strong source at the innermost edge of the broad injection region. This source is most likely a region of direct ionospheric injection.

In addition to substorm ion injection, SC-8 data have been used to investigate injection and convection at the time of magnetospheric storms. Ionospheric plasma injection was studied during a storm period using data from both S3-3 and SCATHA (Strangeway and Johnson, 1984). Large amounts of ionospheric plasma were observed at both spacecraft around the main phase of the storm and, at SCATHA, O^+ was found to be a major component in terms of both density and energy density. Radially dependent features observed in the S3-3 data were explained by convection and time of flight effects, and SCATHA observations were used to infer multiple injections of plasma on the nightside.

Detailed Structure of Plasma Distributions

The sometimes highly time-dependent waves and fields which take part in the energization and transport of magnetospheric plasmas often leave distinct signatures in the particle distribution functions. A detailed investigation of such signatures in various ion species can provide valuable knowledge about these processes - even those which may occur at some distance from the point of observation.

One very common distribution consists of field-aligned ions at energies below several keV, with more energetic ions having peak fluxes at 90 degrees pitch angle. SC-8 data have shown that the low energy portion of this "zipper distribution" is dominated by O^+ , while H^+ dominates the higher energies (Kaye et al., 1981b). These data imply an ionospheric source for the low energy field-aligned ions and a plasma sheet source at higher energies.

In addition to the fairly stable field-aligned ions seen in the zipper distribution, short-lived bursts were also observed (Kaye et al., 1981a). The bursts were predominately O^+ with some H^+ and had characteristic lifetimes of minutes. Average burst energy was near 1 keV and the pitch angle width was typically 5-25 degrees. The data suggested that significant velocity space diffusion affected the burst ions at latitudes near the geomagnetic equator.

An exception to the usual rule of field-aligned ions at low energies is the highly anisotropic, very intense population of ions which is sometimes observed within a few degrees of the geomagnetic equator. SCATHA observations found that these ions are dominated by protons at energies above the measurement limit of 100 eV (Quinn and Johnson, 1982). The composition of these ions was somewhat surprising in that previous theoretical work had suggested that wave heating processes would leave an equatorial population of He^+ . In fact, the He^+

component of the equatorially trapped population was not significant in any of the 8 cases studied.

The observed variations in measured ion distributions due to interactions with a large scale hydromagnetic wave were used to investigate both the radial gradient of ion phase space density and properties of the wave itself (Kaye and Shelley, 1981). It was found for the case studied that the radial gradient of phase space density was negative for both H^+ and O^+ , and that the spatial scale length of the gradient was several earth radii. The deduced azimuthal wave electric field of approximately 10 mV/m was sufficient to displace plasma about 1.5 earth radii during an oscillation.

The Hot Plasma Environment and Spacecraft Interactions

There is a good deal of interest among spacecraft designers and operators, as well as within the scientific community, in obtaining an accurate specification of the space environment and in understanding the interactions of this environment with spacecraft systems. Ion composition data are required to understand surface interactions and to properly determine ambient densities. One particularly important spacecraft-environment interaction is the electrostatic charging and discharging of surfaces (dominated by particles with energies below a few keV) and of internal dielectrics (dominated by more energetic particles). The SCATHA data have been analyzed to provide specific information on the environment with regard to spacecraft interactions (Johnson, 1981; Sharp et al., 1984). Also, the composition of ion fluxes to the spacecraft during a charging event have been studied (Johnson et al., 1981).

Syntheses of Ion Composition Results

The many topical areas of investigation described above are complemented by contributions of the SC-8 data to the broader picture of magnetospheric processes. The circulation of energetic ions of terrestrial origin has been analyzed using data from several spacecraft with the capability to make composition measurements (Shelley, 1984). A review paper: "Hot Plasma Composition Results from the SCATHA Spacecraft" summarizes contributions of the SC-8 instrument (Johnson et al., 1983). Contributions of SCATHA composition data to the International Magnetospheric Study have also been recently reviewed (Quinn and Shelley, 1984).

Publications Supported by ONR Contract N00014-76-C-0444

Davidson, G.T., P. Filbert, and R.W. Nightingale, Observations of Intense Trapped Electron Fluxes at Synchronous Altitudes, to be submitted to J. Geophys. Res., 1984.

Filbert, P.C., J.B. Reagan, R.W. Nightingale, E.E. Gaines, G.T. Davidson, and W.L. Imhof, Coordinated Observations of Precipitating Energetic Electrons at High and Low Altitudes Using the SCATHA and P78-1 Satellites, to be submitted to J. Geophys. Res., 1984.

Gaines, E.E., R.W. Nightingale, W.L. Imhof, and J.B. Reagan, Enhanced Radiation Doses to High-Altitude Spacecraft During June 1980, IEEE Trans. of Nucl. Sci., NS-28, p. 4502, 1981.

Imhof, W.L., J. Stadsnes, J.R. Kilner, D.W. Datlowe, G.H. Nakano, J.B. Reagan, and P. Stauning, Mapping of Energetic Electron Precipitation Following Substorms Using the Satellite Bremsstrahlung Technique, J. Geophys. Res., 87, p. 671, 1982a.

Imhof, W.L., J. Stadsnes, J.B. Reagan, J.R. Kilner, E.E. Gaines, D.W. Datlowe, J. Mobilia, and G.H. Nakano, Satellite Bremsstrahlung X-Ray Measurements at the Onset of a Magnetospheric Substorm, J. Geophys. Res., 87, p. 8149, 1982b.

Johnson, R.G., Review of Hot Plasma Composition Near Geosynchronous Altitude, in Spacecraft Charging Technology 1980, Conference Proceedings, ed. N.J. Stevens and C.P. Pike, NASA CP 2182, p. 412, 1981.

Johnson, R.G., R. Strangeway, S. Kaye, R. Sharp, and E. Shelley, SCATHA

Observations of Space Plasma Composition During a Spacecraft Charging Event, in
Spacecraft Charging Technology 1980, Conference Proceedings, ed. N.J. Stevens
and C.P. Pike, NASA CP 2182, p. 433, 1981.

Johnson, R.G., R.J. Strangeway, E.G. Shelley, J.M. Quinn, and S.M. Kaye, Hot
Plasma Composition Results from the SCATHA Spacecraft, in Energetic Ion
Composition in the Earth's Magnetosphere, ed. R.G. Johnson, p. 287, Terra
Scientific Publishing, 1983.

Kaye, S.M. and E.G. Shelley, The Radial Gradient of 0.1- to 32-keV H⁺ and O⁺ and
the Azimuthal Wave Electric Field as Inferred From a Large-Scale Dayside
Pulsation, J. Geophys. Res., 86, p. 2455, 1981.

Kaye, S.M., R.G. Johnson, R.D. Sharp, and E.G. Shelley, Observations of
Transient H⁺ and O⁺ Bursts in the Equatorial Magnetosphere, J. Geophys. Res.,
86, p. 1335, 1981a.

Kaye, S.M., E.G. Shelley, R.D. Sharp, and R.G. Johnson, Ion Composition of
Zipper Events, J. Geophys. Res., 86, p. 3383, 1981b.

Quinn, J.M. and R.G. Johnson, Composition Measurements of Warm Equatorially
Trapped Ions Near Geosynchronous Orbit, Geophys. Res. Lett., 9, p. 777, 1982.

Quinn, J.M. and R.G. Johnson, Observations of Ionospheric Source Cone
Enhancements at the Substorm Injection Boundary, submitted to J. Geophys. Res.,
1984.

Quinn, J.M. and E.G. Shelley, Results of the SCATHA Ion Composition Experiment During the IMS, in Proceedings of the Symposium on the 'Achievements of the IMS', ESA Publication, in press, 1984.

Reagan, J.B., R.W. Nightingale, E.E. Gaines, W.L. Imhof, and E.G. Stassinopoulos, Outer Zone Energetic Electron Spectral Measurements, J. Spacecraft and Rockets, 18, p. 83, 1981a.

Reagan, J.B., R.W. Nightingale, E.E. Gaines, R.E. Meyerott, and W.L. Imhof, Role of Energetic Particles in Charging/Discharging of Spacecraft Dielectrics, in Spacecraft Charging Technology 1980, Conference Proceedings, ed. N.J. Stevens and C.P. Pike, NASA CP 2182, p. 74, 1981b.

Reagan, J.B., R.E. Meyerott, E.E. Gaines, R.W. Nightingale, P.C. Filbert, and W.L. Imhof, "Space Charging Currents and Their Effects on Spacecraft Systems, IEEE Trans. on Elec. Insul., EI-18, p. 354, 1983.

Sharp, R.D., W. Lennartsson, and R.J. Strangeway, The Ionospheric Contribution to the Plasma Environment in Near-Earth Space, submitted to Radio Science, 1984.

Shelley, E.G., Circulation of Energetic Ions of Terrestrial Origin in the Magnetosphere, Advances in Space Res., submitted 1984.

Stevens, J.R. and A. L. Vampola (eds), Description of the Space Test Program P78-2 Spacecraft and Payloads, SAMSO TR-78-24, 1978.

**Strangeway, R.J. and R.G. Johnson, Mass Composition of Substorm-Related
Energetic Ion Dispersion Events, J. Geophys. Res., 88, p. 2057, 1983a.**

**Strangeway, R.J. and R.G. Johnson, On the Injection Boundary Model and
Dispersing Ion Signatures at Near-Geosynchronous Altitudes, Geophys. Res. Lett.,
10, p. 549, 1983b.**

**Strangeway, R.J. and R.G. Johnson, Energetic Ion Mass Composition as Observed at
Near-Geosynchronous and Low Altitudes During the Storm Period of February 21 and
22, 1979, J. Geophys. Res., 89, p. 8919, 1984.**

APPENDIX 1

**Description of The High Energy
Particle Spectrometer (SC-3)**

DESCRIPTION OF THE SPACE TEST PROGRAM P78-2 SPACECRAFT AND PAYLOADS

EDITED BY
JOHN R. STEVENS
AND
ALFRED L. VAMPOLA

9. SC3 HIGH ENERGY PARTICLE SPECTROMETER

9.1 SCIENTIFIC OBJECTIVES

The primary goals of the SC3 payload are to make energetic electron and proton measurements that are needed to meet the objectives of the spacecraft charging program. The energetic electron flux at near-synchronous altitudes exhibits pronounced pitch-angle, diurnal and solar rotation dependences, and is highly dynamic in time. The energetic electrons behave differently in many ways from the low-energy electrons and, therefore, measurements obtained with the SC3 spectrometer will complement the measurements made at lower energies by other experiments on the P78-2 spaceflight. One application to the spacecraft charging mission is the measurement of flux intensities of penetrating energetic

electrons to determine whether anomalous charging of coaxial cables in spacecraft is a source of system noise.

A knowledge of the fluxes, spectra, and pitch-angle distributions of the energetic electrons at near-equatorial altitudes on high L-shells is essential to an understanding of environmental effects on ELF and VLF communications. These communications are affected by naturally-occurring and artificially-induced wave-particle interactions through transfer of wave energy to particle energy. Perturbation of the particle energy or pitch-angle distribution as a result of such interactions enhances particle precipitation from the radiation belts, which

SUBSEQUENTLY AFFECTS LONG-WAVELENGTH COMMUNICATION SYSTEMS ADVERSELY. PAYLOADS ON THE P78-2 SPACEFLIGHT SIMULTANEOUSLY MEASURE THE DETAILED PARAMETERS OF THE ENERGETIC ELECTRON POPULATION, THE COLD PLASMA ENVIRONMENT, AND THE ELECTRIC AND MAGNETIC FIELD ENVIRONMENT NEAR-SYNCHRONOUS EQUATORIAL ALTITUDES AT ALL LOCAL TIMES UNDER A VARIETY OF NATURALLY-OCCURRING WAVE CONDITIONS. THE SC3 SPECTROMETER, IN CONJUNCTION WITH LOW ENERGY ELECTRON MEASUREMENTS IN THE SC5 AND SC9 PAYLOADS, WILL DEFINE THE TRAPPED ELECTRON ENVIRONMENT THAT INTERACTS WITH THE WAVE ENVIRONMENT AS MEASURED BY THE ELECTRIC AND MAGNETIC FIELD PAYLOADS, SC1, SC10, AND SC11, UNDER WELL-DEFINED COLD PLASMA CONDITIONS THAT ARE MEASURED BY THE SC6 AND SC7 PAYLOADS. THE KNOWLEDGE OBTAINED FROM SUCH A SIMULTANEOUS STUDY SHOULD LEAD TO A BETTER UNDERSTANDING OF BOTH NATURAL AND MAN-MADE ELF AND VLF WAVE INTERACTIONS WITH TRAPPED PARTICLES IN THE MAGNETOSPHERE AND TO THE SUBSEQUENT EFFECTS OF SUCH INTERACTIONS ON THE IONOSPHERE.

THE SC3 PAYLOAD WILL MEASURE THE ELECTRON ENVIRONMENT WITH GOOD ENERGY RESOLUTION IN THE ENERGY REGION (1.5 MEV) AT THE TIME OF SOLAR MAXIMUM CONDITIONS. THE ENERGETIC ELECTRONS IN THIS ORBIT CONSTITUTE A POTENTIAL HAZARD TO THE ELECTRONIC COMPONENTS USED IN BOTH THE PAYLOADS AND THE SPACECRAFT. OUTPUTS FROM THE SC3 PAYLOAD WILL BE USED TO DETERMINE IN NEAR REALTIME THE ENVIRONMENT AND RADIATION DOSE ACQUIRED BY THE SPACECRAFT BEHIND VARIOUS SHIELDING THICKNESS. THESE DATA WILL BE USED FOR THE P78-2 SPACEFLIGHT DEGRADATION CALCULATIONS AND TO IMPROVE THE RADIATION MODELS FOR SUBSEQUENT MISSIONS.

AT THE TIMES OF SOLAR PARTICLE EVENTS THAT REACH THE EARTH, ENERGETIC SOLAR PROTONS, ELECTRONS, AND ALPHA PARTICLES TYPICALLY HAVE HIGHLY EFFICIENT ACCESS TO THE NEAR-GEOSYNCHRONOUS ORBIT. THEY MAY SIGNIFICANTLY ALTER THE ENERGETIC PLASMA COMPOSITION. THE SC3 SPECTROMETER WILL MEASURE THESE ENERGETIC SOLAR PARTICLES AND THEIR CONTRIBUTIONS TO THE BACKGROUNDS AND RADIATION DOSE IN THE OTHER ELEMENTS OF THE P78-2 SPACEFLIGHT. THE SC3 INSTRUMENT MEASURES THE FLUXES, SPECTRA, AND PITCH-ANGLE DISTRIBUTION OF THE ENERGETIC PLASMA IN THE ENERGY RANGE 50 KEV TO

5100 KEV AND THE INTEGRAL FLUX BETWEEN 5100 KEV AND 10,000 KEV. IN ADDITION, THE INSTRUMENT MEASURES THE PROTON ENVIRONMENT AT ENERGIES BETWEEN 1-200 MEV AND THE ALPHA PARTICLE ENVIRONMENT BETWEEN 6-60 MEV DURING SOLAR PARTICLE EVENTS. THE MEASUREMENTS ARE MADE WITH A PITCH ANGLE RESOLUTION OF 3 DEG (FULL-WIDTH-AT-HALF-MAXIMUM). THE ENERGY SPECTRA ARE OBTAINED WITH A 12-CHANNEL PULSE HEIGHT ANALYZER THAT CAN BE PROGRAMMED BY COMMAND TO COVER A NARROW OR WIDE ENERGY RANGE. IN THIS MANNER, BOTH COMPLETE SURVEY DATA AND HIGH RESOLUTION SPECTRAL DATA CAN BE OBTAINED ON COMMAND.

9.2 MEASURING TECHNIQUE

THE BASIC MEASUREMENT TECHNIQUE IS A SOLID-STATE PARTICLE SPECTROMETER CONSISTING OF FOUR SENSOR ELEMENTS. A LINE DRAWING OF THE SPECTROMETER IS SHOWN IN FIGURE 9.1. VARIOUS LOGIC COMBINATIONS OF THE FOUR SENSORS IN THE INSTRUMENT ARE USED TO DETERMINE THE PARTICLE TYPES AND ENERGY RANGES. THE VARIOUS PARTICLE TYPES AND ENERGY RANGES ARE MEASURED IN SEVERAL TIME-MULTIPLEXED MODES OF OPERATION THAT ARE COMMAND-SELECTABLE.

THE D-DETECTOR, WHICH IS $200\mu\text{m}$ THICK INTRINSIC Si, IS USED TO MEASURE BOTH THE RATE OF ENERGY LOSS OF THE HIGHER ENERGY PARTICLES AND TO DIRECTLY STOP AND MEASURE THE LOWER ENERGY PARTICLES. THE E-DETECTOR, WHICH CONSISTS OF FIVE 2 MM THICK DETECTORS IN PARALLEL, IS LOCATED BEHIND THE D-DETECTOR TO STOP THE HIGHER ENERGY PARTICLES AND TO MEASURE THEIR TOTAL ENERGY LOSS. THE E'-DETECTOR, WHICH IS 1000 MICRONS THICK, IS LOCATED BEHIND THE E-DETECTOR AND IS USED AS AN ACTIVE COLLIMATOR. BEHIND THE E'-DETECTOR IS A TUNGSTEN ABSORBER THAT SETS THE UPPER ENERGY LIMIT FOR ANALYSIS. ALL OF THESE DETECTORS ARE FABRICATED OF SURFACE-BARRIER SILICON AND ARE STACKED TOGETHER IN A TELESCOPE CONFIGURATION. THE ENTIRE STACK IS SURROUNDED BY THE A-DETECTOR, WHICH CONSISTS OF PLASTIC SCINTILLATOR VIEWED BY A PHOTOMULTIPLIER TUBE. THE PURPOSE OF THE A-ANTICOINCIDENCE DETECTOR IS TO SENSE AND REJECT ENERGETIC PARTICLES AND BREMSTRAHLUNG THAT PENETRATE EITHER THE OUTER SHIELDING WALLS OF ALUMINUM AND TUNGSTEN OR THE SILICON DETECTOR STACK AND ABSORBER. THE SENSOR STACK IS LOCATED

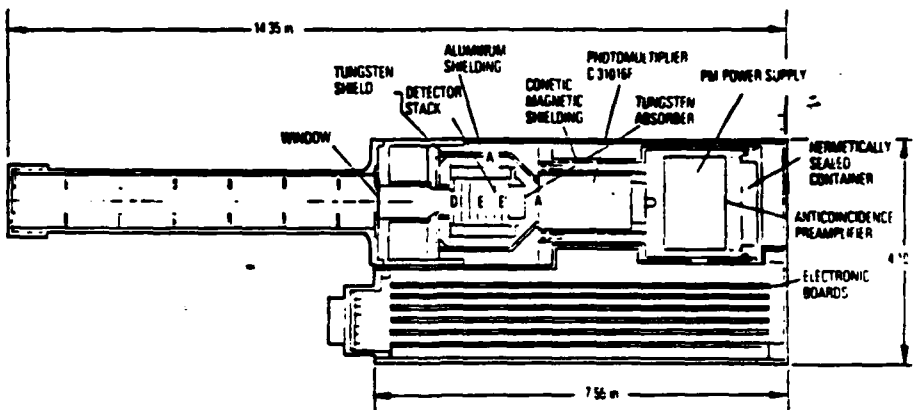


Figure 9.1. SC3 High Energy Particle Spectrometer

BEHIND A LONG, NARROW COLLIMATOR THAT DEFINES THE 3 DEG FIELD OF VIEW.

9.3 FUNCTIONAL BLOCK DIAGRAM

A FUNCTIONAL BLOCK DIAGRAM OF THE SC3 INSTRUMENT IS SHOWN IN FIGURE 9.2. THE INSTRUMENT OPERATES FROM A 2048-BIT SEMICONDUCTOR MEMORY (CMOS) THAT IS STRUCTURED INTO 256 8-BIT WORDS THAT ARE INDIVIDUALLY ADDRESSABLE AND LOADABLE VIA 9-BIT SERIAL-DIGITAL COMMANDS (MAGNITUDE COMMANDS). FOUR OF THESE WORDS (32-BIT CONTROL REGISTER) COMPLETELY DEFINE ONE OPERATING MODE OF THE INSTRUMENT. A MODE IS DEFINED BY SPECIFYING THE LOGIC CONDITIONS (COINCIDENCE/ANTICOINCIDENCE), GAIN, AND ENERGY THRESHOLDS REQUIRED BETWEEN THE FOUR SENSOR ELEMENTS (D, E, E', A) TO UNIQUELY ESTABLISH A PARTICLE TYPE AND ENERGY RANGE FOR ANALYSIS. A CHOICE OF TWO AMPLIFIER GAIN SETTINGS FOR THE D- AND E-DETECTORS IS AVAILABLE. THE LOWER AND UPPER ENERGY THRESHOLDS SELECTED FOR ANALYSIS BY THE 12-CHANNEL PULSE-HEIGHT-ANALYZER (PHA) ARE DETERMINED TO 8-BIT AND 6-BIT RESOLUTION, RESPECTIVELY. EITHER THE D- OR E-DETECTOR IS SELECTABLE AT ANY TIME FOR ANALYSIS BY THE PHA THROUGH THE MULTIPLEXER. THE ENERGY THRESHOLD OF THE SENSOR NOT SELECTED FOR ANALYSIS CAN BE SET TO 8-BIT RESOLUTION.

EIGHT OF THESE MODES COMprise ONE PAGE OF MEMORY AND EIGHT PAGES CONSTITUTE THE COMPLETE MEMORY. TO LOAD THE COMPLETE MEMORY REQUIRES 512 COMMANDS (ADDRESS + DATA) AND 512 SECONDS AT A COMMANDING RATE OF ONE PER SECOND. EACH PAGE OF MEMORY CAN BE STRUCTURED TO EMPHASIZE ONE PARTICLE TYPE (I.E., ELECTRONS) OR ALL PARTICLE TYPES; TO

CONCENTRATE ON SPECIAL EVENTS, SUCH AS SOLAR PARTICLE EVENTS; OR TO DWELL ON A NARROW ENERGY REGION OF INTEREST WITH ANY PARTICLE TYPE. THE COMMANDABLE OPTIONS ARE EXTENSIVE BUT AN OPTIMUM OPERATING CONFIGURATION WILL BE LOADED INITIALLY AND ADJUSTED AS CONDITIONS DICTATE.

ONCE THE INSTRUMENT MEMORY IS LOADED, OPERATION FROM ANY PAGE IS SELECTABLE BY A SUBSEQUENT INSTRUCTION MAGNITUDE COMMAND (INST). EACH 9-BIT INST COMMAND ALSO SELLECTS THE DWELL TIME THAT THE INSTRUMENT WILL REMAIN IN EACH MODE AS IT CYCLES THROUGH THE MEMORY PAGE. TIMES OF 8, 16, 32, AND 64 SEC ARE POSSIBLE. SINCE THE SATELLITE SPIN RATE IS 1 RPM, THE LONGEST DWELL TIME CORRESPONDS APPROXIMATELY TO ONE SPIN PERIOD. DWELL TIMES AS SHORT AS ONE-EIGHTH OF A SPIN PERIOD ARE, THEREFORE, ALSO POSSIBLE. THE ABILITY TO CALIBRATE THE INSTRUMENT WITH AN INTERNAL PULSE GENERATOR SYSTEM IS SELECTABLE BY ONE BIT OF THE INST COMMAND. THE ORDER OF THE DIGITAL DATA OUTPUT FROM THE SPECTROMETER IS ALSO SELECTABLE. A PRIMARY FORMAT IS USED UNLESS SOME FAILURE OCCURS IN THE READOUT CIRCUITRY AT WHICH TIME A SECONDARY FORMAT IS AVAILABLE. THE ABILITY TO SELECT A HARDWIRED BACKUP MODE IS ALSO AVAILABLE SHOULD A MAJOR FAILURE OCCUR IN THE MEMORY OPERATION. THE HARDWIRED BACKUP MODE MEASURES THE HIGHER ENERGY ELECTRONS (300-5100 KEV) AND IS INDEPENDENT OF THE MEMORY. THE INSTRUMENT OPERATES IN THIS CONDITION AUTOMATICALLY WHENEVER THE MEMORY IS BEING LOADED OR DISABLED. DIGITAL SIGNALS FROM THE FOUR SENSORS ARE APPLIED TO A COINCIDENCE LOGIC UNIT WHERE THEY ARE TESTED AGAINST THE CONDITIONS SPECIFIED IN THE COMMAND TO

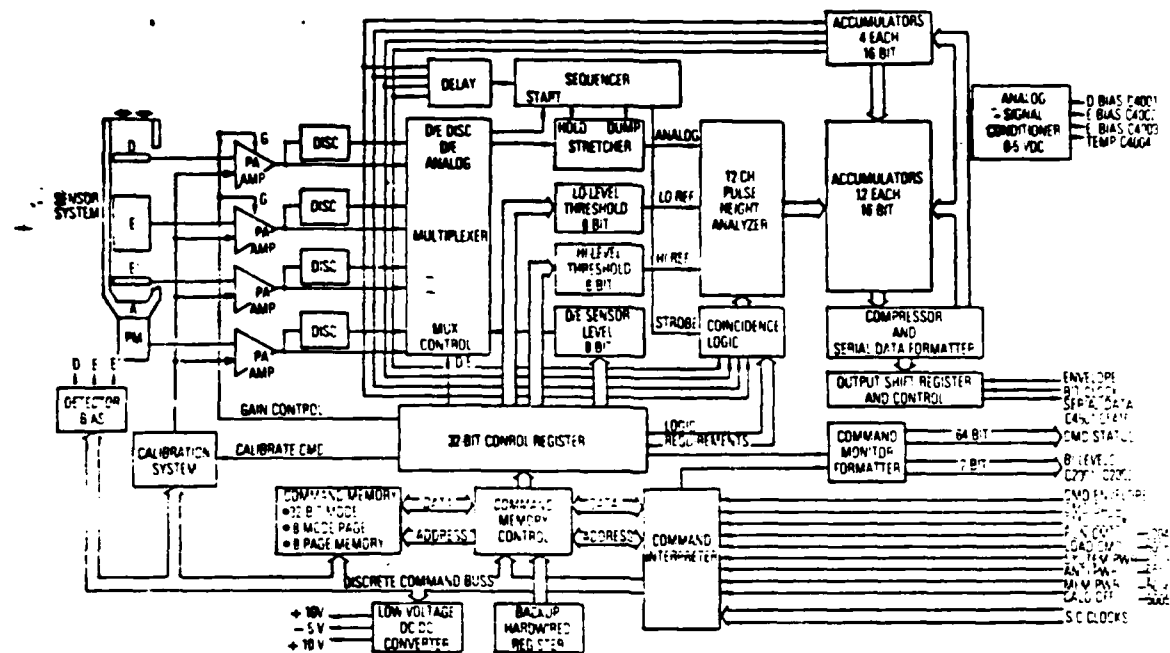


Figure 9.2. Functional Block Diagram

UNIQUELY MEASURE A CERTAIN PARTICLE TYPE AND ENERGY RANGE. THE LOGIC CONDITIONS REQUIRED TO MEASURE THE VARIOUS PARTICLES AND ENERGIES OF INTEREST ARE SHOWN IN TABLE 9.1. THE SUBSCRIPTS ON THE SENSOR NOTATION REFER TO THE LOWER ENERGY THRESHOLDS REQUIRED TO ESTABLISH THE CORRECT ENERGY RANGE. HIGH AMPLIFIER GAIN IS REQUIRED IN THE ELECTRON MODES OF OPERATIONS SINCE THE ENERGIES INVOLVED ARE CONSIDERABLY BELOW THOSE OF THE PROTONS AND ALPHA PARTICLES MEASURED. BARS OVER A SENSOR NOTATION INDICATE AN ANTICOINCIDENCE CONDITION (NO SIGNAL) MUST BE PRESENT FROM THAT SENSOR TO SATISFY THE LOGIC. THE PLASTIC SCINTILLATOR, A, IS ALWAYS USED IN AN ANTICOINCIDENCE MODE. THE E'-DETECTOR IS USED TO DETECT AND MEASURE THE ENERGETIC ELECTRONS BETWEEN 5100 AND 10,000 keV, WHERE THE UPPER ENERGY IS DETERMINED BY THE TUNGSTEN ABSORBER BEHIND THE SENSOR AND IN FRONT OF THE ANTICOINCIDENCE SCINTILLATOR (FIGURE 9.1). THE E'-DETECTOR IS ALSO USED TO DETECT AND COLLIMATE THE HIGHEST ENERGY PROTONS BUT ANALYSIS IS PERFORMED IN THE NONLINEAR PORTION OF THE E-DETECTOR.

SIGNALS FROM THE SENSOR SELECTED FOR ANALYSIS THAT SATISFY ALL THE LOGIC CONDITIONS ARE ROUTED TO THE 12-CHANNEL DIFFERENTIAL PHA AFTER BEING STRETCHED

IN TIME. THE PHA IS A 13-LEVEL COMPARATOR STACK WITH THE LOWER AND UPPER LEVEL REFERENCES DETERMINED BY COMMAND. THE LOWER LEVEL REFERENCE CAN BE SET TO 1-PART-IN-256 (8-BIT) OF THE AMPLIFIER RANGE WHILE THE UPPER LEVEL CAN BE SET AND RESOLVED TO 1-PART-IN-64 (6-BIT) OF THE RANGE. ALL AMPLIFIER PULSES BETWEEN THE LOWER AND UPPER REFERENCE LEVELS ARE ANALYZED INTO 12 EQUAL-WIDTH VOLTAGE BINS. BASIC ANALYSIS TIME IS 496 MSEC. THE REFERENCE LEVELS CAN BE SET AS CLOSE AS THE BASIC RESOLUTION AND STABILITY OF THE PHA SYSTEM (1-PART-IN-256) IN ORDER TO ACHIEVE HIGH ENERGY RESOLUTION OVER A LIMITED ENERGY RANGE. ALTERNATELY, THE LEVELS CAN BE SET OVER A WIDER RANGE WITH BROADER ENERGY RESOLUTION IN ORDER TO OBTAIN BETTER STATISTICS.

Table 9.1. Detector Logic

Detector	Particle Measured	Energy Range	Detector Logic	Detector Analysis	Comments
Elect 1	Electrons	50-100 keV	D ₁ , E ₁ , E' ₁ , A	D ₁	No Amplifier Gain E ₁ = 100 keV
Elect 2	Electrons	100-1100 keV	B ₁ , E ₁ , E' ₁ , A	E ₁	No Amplifier Gain E ₁ = 1100 keV
Elect 3	Electrons	1100-10000 keV	B ₁ , E ₁ , E' ₁ , A	E ₁	Differential channels E ₁ = 1100 keV
Proton 1	Protons	1-0.5 MeV	B ₂ , E ₂ , E' ₂ , A	D ₂	D ₂ = 0.5 MeV E ₂ = 174 MeV
Proton 2	Protons	1-1.5 MeV	B ₂ , E ₂ , E' ₂ , A	E ₂	E ₂ = 1.5 MeV
Proton 3	Protons	30-40 MeV	B ₃ , E ₃ , E' ₃ , A	E ₃	E ₃ = 10 MeV
Proton 4	Protons	60-80 MeV	B ₃ , E ₃ , E' ₃ , A	E ₄	E ₄ = 1.5 MeV
Alpha 1	Alpha	6-8 MeV	B ₄ , E ₁ , E' ₁ , A	D ₄	D ₄ = 1.5 MeV

Each of the 12 channels of the PHA are connected to 16-bit binary accumulator shift registers that are readout every 0.5 sec to the telemetry. The 0.5-sec accumulation time corresponds to a 3-deg rotation of the satellite. In addition, there are 16-bit accumulators connected to each of the four sensors to measure the integral counting rates above the lowest threshold.

Upon serial readout, each 16-bit accumulator is compressed into an 8-bit output word in a pseudo-logarithmic manner. The 8-bit output word consists of 4 bits that define the location of the most-significant-one bit in the accumulator (a fifth bit is implied) and the 4 bits of binary data that follow. The data contents of the accumulator up to a value of 31 are not compressed and, hence, are not effected in accuracy. At higher accumulator values the maximum error associated with the truncation never exceeds a few percent.

A 64-bit status block describing the complete configuration logic of the instrument is readout every 8 sec and, therefore, the minimum dwell time (8 sec) of a mode can be defined. This status block reflects the control logic of the instrument as acquired from the memory for each mode and also the conditions specified by the instruction and the discrete commands. Four analog outputs measure the bias on the D-, E-, and E'-detectors and the temperature of these detectors. A summary of the key features of the spectrometer is given in Table 9.2.

Table 9.2. Summary of the Key Features of the SC3 Spectrometer

Number of sensors	4
Particles and energy range measured	e p e
	50-5100 keV, 5-10.0 MeV 1-200 MeV 6-60 MeV
Number of differential energy channels	12
Energy resolution	Programmable
Number of integral energy channels	4
Time required to obtain an integral or a differential spectra	500 ms
Pitch angle resolution	3° (FWHM)
Geometric factor	$\sim 3 \times 10^{-3} \text{ cm}^2 \cdot \text{sr}$
Number of MODES of operation (to measure all particles and energies)	8
Dwell time in each MODE	8, 16, 32, 64 sec (programmable)

9.4 OPERATIONAL ASPECTS

The SC3 instrument utilizes three discrete commands to power (1) the instrument (5003), (2) the anticoincidence system (5002), and (3) the memory system (5006). A LOAD command (5008) must precede each memory loading operation and a RUN command (5004) must precede the sending of an INSTRUCTION (INST) command. There are 256 INST commands available for use (5101 through 5356). The CALIBRATION system can be disabled in the event of a failure via a discrete command (5005). The SC3 memory will be loaded at the earliest opportunity after launch and remain active for the duration of the mission. This is accomplished by sending 256 combinations of data and address words at a rate of 1 word/sec. Changes to the memory will be accomplished by automatic blocks of serial binary commands (9 bit) or by individual serial commands (9 bit). Threshold changes to select different energy ranges are expected to be the most frequently sent command after payload initialization.

It is planned that the SC3 instrument be operational at all times during the P78-2 spaceflight. The primary mode of operation will be measuring electrons and the instrument will operate alternately between the mid- and high-energy electron ranges from a page of memory. These data will be used in near-realtime analysis to determine the primary energy spectrum and radiation dose acquired behind various shielding thicknesses. At the times of solar particle events, operation will be by command from a preselected page in memory to obtain the proton spectrum and its contribution to the dose.

Since a knowledge of the SC3 orientation with respect to the magnetic field orientation is essential to all measurements, the SC3 instrument will be operated with the SC11 instrument. Special alignment calibrations between the two instruments will be performed on-orbit.

APPENDIX ?

**Description of The Energetic Ion
Composition Experiment (SC-8)**

DESCRIPTION OF THE SPACE TEST PROGRAM P78-2
SPACECRAFT AND PAYLOADS

EDITED BY
JOHN R. STEVENS
AND
ALFRED L. VAMPOLA

15. SC8 ENERGETIC ION COMPOSITION EXPERIMENT

15.1 SCIENTIFIC OBJECTIVES

The Energetic Ion Composition Experiment, SC8, measures the mass composition of the hot plasmas enveloping the P78-2 spacecraft. The ion flux measurements span the energy region from 100 eV to 32 keV and the mass range from 1 to greater than 160 amu.

The objectives of the experiment fall into two general categories: (A) Spacecraft charging phenomena, and (B) plasma interaction processes. The SC8 experiment supports understanding the spacecraft charging phenomena in several ways. (1) The composition and spatial anisotropies of the positive ions in the ambient hot plasma that is required to understand and to model the sheath region around the spacecraft during charging events is determined. (2) The photoionized gaseous and ion contaminants emitted by the spacecraft (which has been observed previously on

ATS-5 and ATS-6 without mass identification) are measured. (3) The ion composition of the plasma prior to charging events is measured in order to assess the capabilities for predicting charging events on the reconfiguration of the magnetospheric current system prior to the onset of geomagnetic substorms. (4) Temporal and radial dependencies of the plasma composition are determined to aid in modeling the hot plasma environment for satellite orbits at higher and lower altitudes and inclinations than the P78-2 spacecraft orbit. (5) Finally, selected plasma conditions are measured during which ion fluxes from the SC4 ion gun are returned to the spacecraft.

The SC8 experiment supports understanding the plasma interaction processes in several ways. (1) Plasma and field conditions that produce ionospheric ion acceleration will be

INVESTIGATED. (2) THE LOCAL TIME AND GEOMAGNETIC LATITUDE DISTRIBUTIONS OF THE SOURCE REGIONS OF FIELD-ALIGNED IONOSPHERIC IONS WILL BE INVESTIGATED. (3) THE PLASMA AND FIELD CONDITIONS THAT PRODUCE THE PRECIPITATION OF ENERGETIC PARTICLES FROM THE TRAPPED POPULATIONS WILL BE INVESTIGATED. (4) THE LARGE-SCALE AND SMALL-SCALE TRANSPORT PROCESSES FOR THE HOT PLASMAS WILL BE INVESTIGATED. (5) FINALLY, THE PLASMA AND FIELD CONDITIONS THAT RESULT IN VLF WAVE GENERATION AND AMPLIFICATION IN THE MAGNETOSPHERE WILL BE INVESTIGATED.

15.2 MEASURING TECHNIQUE

THE S08 INSTRUMENT IS AN ENERGETIC ION MASS SPECTROMETER CONTAINING THREE PARALLEL ANALYZER UNITS, EACH OF WHICH MEASURES IONS IN A DIFFERENT ENERGY REGION OF THE RANGE FROM 0.1 TO 32 KEV. EACH UNIT CONSISTS OF A CROSSED ELECTRIC AND MAGNETIC FIELD VELOCITY FILTER (WEIN FILTER) IN SERIES WITH AN ELECTROSTATIC ANALYZER (ESA) AND A CHANNEL ELECTRON MULTIPLIER SENSOR. ONE OF THE UNITS IS SHOWN SCHEMATICALLY IN FIGURE 15.1.

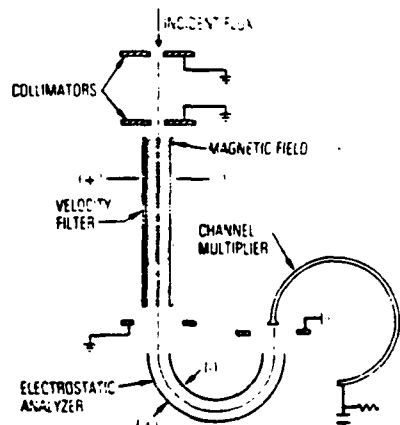


Figure 15.1. Ion Mass Spectrometer

THE INSTRUMENT HAS TWO BASIC MODES OF OPERATION AND TWO MASS RANGES OF COVERAGE IN EACH MODE. THE TWO MASS RANGES COVER FROM APPROXIMATELY 0.8 TO 80 AMU(NORMAL) AND 12 AMU TO GREATER THAN 160 AMU (HEAVY). IN THE FIRST OPERATING MODE, EACH OF THE THREE ANALYZER UNITS CYCLES THROUGH FOUR DISCRETE ESA SETTINGS IN 16 SEC, REMAINING FIXED FOR 2 SEC AT EACH SETTING. DURING EACH 2-SEC PERIOD, THE VELOCITY FILTER VOLTAGE IS RAMPED TO PROVIDE A 32-POINT MASS-PER-UNIT-CHARGE (M/Q) SPECTRUM OVER

ONE OF THE TWO RANGES INDICATED ABOVE. Thus, a full mass spectrum is obtained at each of 24 energy points every 16 sec. In the second mode, the velocity filter is locked in one of four discrete values corresponding to $M/Q = 1, 2, 4, \text{ or } 16$ for 16 sec, while each ESA is cycled among its eight discrete levels. The ESA voltage is switched every 62 msec. Thus, a 24-point energy-per-unit-charge spectrum from the three units is acquired every 1/2 second at a single M/Q position. After 64 sec on a fixed mass value, the instrument spends 64 sec in Mode 1 to provide information on the background levels obtainable from mass regions between the discrete mass peaks. Following this, the velocity filter is locked on a second mass for 64 sec, again followed by 64 sec in Mode 1. This continues through the four discrete M/Q values. Thus, a complete cycle of the second mode requires 512 sec. Variations in the number and timing of the basic energy and mass values can be selected by realtime commands.

THE INSTRUMENT ALSO INCLUDES FOUR BROADBAND ELECTRON CHANNELS FOR PROVIDING ELECTRON BACKGROUND INFORMATION AND FOR GENERAL CORRELATIVE STUDIES WITH THE PLASMA IONS. FIXED MAGNETIC FIELD ANALYZERS FOLLOWED BY CHANNEL ELECTRON MULTIPLIERS SPAN THE ELECTRON RANGE FROM 1.07 TO 24 KEV WITH CENTRAL ENERGIES AT 0.16, 0.73, 3.3, AND 16 KEV.

15.3 FUNCTIONAL BLOCK DIAGRAM

THE DATA FLOW FROM THE INSTRUMENT IS ILLUSTRATED SCHEMATICALLY IN FIGURE 15.2. ALL OF THE OUTPUTS ARE FROM CHANNEL ELECTRON MULTIPLIERS AND THE DATA FROM EACH CHANNEL ARE HANDLED IN AN ANALOGOUS FASHION. EACH SENSOR OUTPUT IS FOLLOWED BY A PULSE AMPLIFIER, SHAPER, AND DISCRIMINATOR PRIOR TO GOING INTO A 16-BIT COUNTER. THE ACCUMULATION AND READ TIMES FOR THE COUNTERS ARE SYNCHRONIZED WITH THE ANALOG FUNCTIONS AND CONTROLLED BY THE INSTRUMENT CONTROL LOGIC AS INDICATED SCHEMATICALLY BY THE CONTROL LOGIC BLOCK. THE INFORMATION IN THE 16-BIT COUNTERS IS LOGARITHMICALLY COMPRESSED TO 8 BITS PRIOR TO BEING READ INTO THE TELEMETRY BIT STREAM BY THE SPACECRAFT DATA MULTIPLEXER.

AN INFLIGHT CALIBRATION SEQUENCE IS INITIATED BY

REALTIME COMMAND THROUGH THE CALIBRATION CONTROL LOGIC. THIS SEQUENCE CHECKS ALL OF THE COUNTERS AND BUFFERS BY PROVIDING PULSES AT A FIXED RATE INTO EACH COUNTER. CHANNEL MULTIPLIER AND

AMPLIFIER PERFORMANCE IS EVALUATED IN THE CALIBRATION SEQUENCE BY STEPPING THE DISCRIMINATOR THROUGH ITS FOUR SELECTABLE LEVELS FOR EACH OF TWO HIGH VOLTAGE SETTINGS OF THE CHANNEL ELECTRON MULTIPLIERS. THE OPERATING LEVEL OF THE DISCRIMINATOR IS SELECTED BY REALTIME COMMAND.

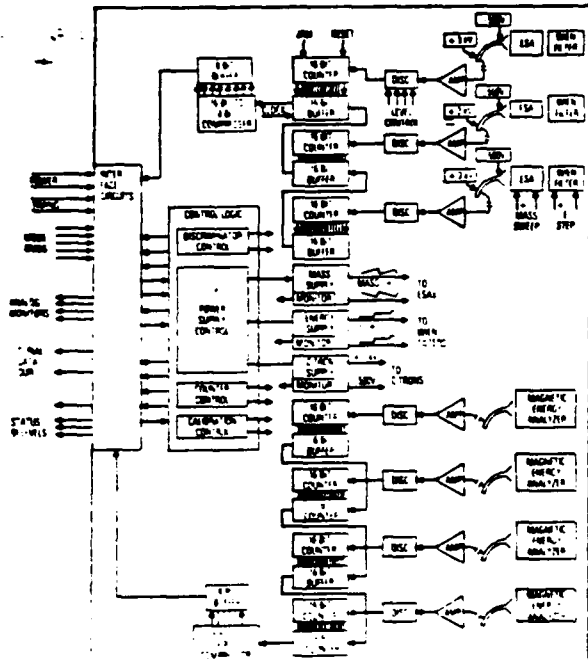


Figure 15.2. Block Diagram

15.4 OPERATIONAL ASPECTS

OPERATING MODES FOR THE INSTRUMENT ARE SELECTED BY REALTIME COMMANDS. AFTER THE INITIAL INSTRUMENT CHECKOUT, IT IS EXPECTED THAT THE INSTRUMENT WILL REMAIN IN A SELECTED MODE FOR AT LEAST 24 HR FOR MOST ROUTINE OPERATIONS. INFLIGHT CALIBRATION OF THE INSTRUMENT WILL BE PERFORMED ABOUT ONCE PER DAY AND IS INITIATED BY REALTIME COMMAND.

DURING THE LIFETIME OF THE SPACECRAFT, MANY DIFFERENT OPERATING MODES WILL BE USED TO INVESTIGATE A WIDE RANGE OF GEOPHYSICAL AND MAN-PRODUCED EVENTS. THESE EVENTS WILL INCLUDE GEOMAGNETIC STORMS AND SUBSTORMS, SOLAR PARTICLE EVENTS, FIELD-ALIGNED ION EVENTS, SOLAR ECLIPSES BY THE EARTH, ION AND ELECTRON GUN OPERATIONS, CHEMICAL RELEASES, AND ELECTROMAGNETIC WAVE INJECTIONS.

APPENDIX 3

Abstracts of Publications

OBSERVATIONS OF INTENSE TRAPPED ELECTRON FLUXES AT SYNCHRONOUS ALTITUDES

G. T. Davidson

P. Filbert

R. W. Nightingale

W. L. Imhof

J. B. Reagan

Lockheed Palo Alto Research Laboratory

3251 Hanover Street

Palo Alto, CA 94304

E. Whipple

University of California at San Diego

ABSTRACT

The Lockheed High Energy Particle Spectrometer on the SCATHA satellite, P78-2, occasionally measures energetic electron fluxes near synchronous altitude that exceed the commonly cited Kennel and Petschek trapping limit. Twelve cases have been analyzed in detail, including several from relatively quiet times and from times when the spectrum became very hard. These were compared with an energy-dependent formulation of the trapping limit [Schulz and Davidson, 1985], which predicts a steeply descending spectrum above the minimum resonant energy for wave growth, and a $1/E$ spectrum at high energies. The spectrometer permitted pitch-angle resolution fine enough to resolve the loss cone and to derive the anisotropies that were needed to make the comparisons with the theory. In all the cases, over a wide range of conditions, there was a region of the spectrum, although often less than a decade wide in energy, that closely matched the theoretical spectrum. The plasma densities derived from the minimum resonant energies were compared with ion densities determined from the UCSD ion spectrometer aboard the SCATHA satellite. The agreement between the two supported the interpretation of the energetic electron spectra. It was concluded that flux limiting may occur much of the time over a portion of the electron spectrum and that the overall spectrum exhibits greater variability than can be simply explained by the flux limiting process. The results were consistent with a model in which the limiting process occurs by sporadic precipitation events, punctuated by intervals of weak diffusion. Numerical estimates of the energy-integrated flux above the minimum resonant energy agreed well with the Kennel and Petschek prediction. A new empirical energy-integrated flux limit of $1 \times 10^{11} / L$ electrons cm^{-2} s^{-1} is suggested.

to be submitted to J. Geophys. Res. 1984.

COORDINATED OBSERVATIONS OF PRECIPITATING ENERGETIC ELECTRONS AT HIGH AND LOW ALTITUDES USING THE SCATHA AND P78-1 SATELLITES

P. C. Filbert, J. B. Reagan, R. W. Nightingale, E. E. Gaines,
G. T. Davidson and W. L. Imhof

Lockheed Palo Alto Research Laboratory
3251 Hanover Street
Palo Alto, CA 94304

ABSTRACT

Energetic electron data from the SCATHA (P78-2) spacecraft in the near-geosynchronous orbit and the low altitude (600 km) polar orbiting P78-1 satellite are presented. The Olson-Pfizer geomagnetic field model was used to determine when the two spacecraft were on the same magnetic drift shell. Temporal flux profiles, differential energy spectra, and pitch-angle distributions from both satellites are compared for three conjunctions which occurred during times of moderate (K_p =3) to intense geomagnetic activity (K_p =6). In addition, a detailed comparison of the SCATHA SC3 electron spectrum at pitch angles which allow the electrons to access the P78-1 orbit is made with a series P78-1 spectra obtained as a function of L-shell. The L-shell with the best spectral agreement is used as an independent determination of magnetic conjugacy in each of the three cases. It is found that in two of the cases the agreement between the model-determined conjugacy and that obtained by the spectral comparison is good even though there was moderate to intense geomagnetic activity at these times. In the third case, a significant difference was found despite the fact that it was the most quiet case and that the measured magnetic field at SCATHA agreed well with the Olsen-Pfizer model. The pitch angle distribution of precipitating energetic electrons measured by P78-1 is used to estimate the pitch-angle diffusion coefficient and the wide-band wave intensity required for resonant scattering using the theory of Kennel and Petschek. The results are compared to SCATHA wave measurements and order of magnitude agreement is found.

to be submitted to J. Geophys. Res., 1984.

Enhanced Radiation Doses to High-Altitude

Spacecraft During June 1980

E. E. Gaines, R. W. Nightingale, W. L. Imhof, and J. B. Reagan
Lockheed Palo Alto Research Laboratory, Palo Alto, Calif.

Abstract

During the period June 9 to 14, 1980 fluxes of high energy electrons were greatly intensified at high altitudes. Since electrons with energies greater than a few MeV can penetrate nominal spacecraft shielding and damage electronic components, the increased fluxes during this period were investigated to determine the nature and extent of damage they might cause to spacecraft in equatorial orbits near an altitude of 30000 km. It is concluded that short term effects such as charging and subsequent discharge in dielectrics from the accumulation of electrons stopped in the material in a period of the order of a day are more likely than total dose damage over the few days duration of high flux levels.

1. Introduction

Fluxes of energetic electrons at high altitudes in the outer radiation belt were intensified to an unusual extent, particularly for energies greater than 1 MeV, by a magnetic storm which began on June 11, 1980. Since electrons with these high energies can penetrate nominal spacecraft shielding and cause damage to electronic components, the fluxes and energy spectra of electrons up to 5 MeV in the time period 9 - 14 June 1980 were investigated. Measurements were made with the high-energy particle spectrometer known as SC-3 on board the USAF Space Test Program P78-2 spacecraft (Spacecraft-Charging-At-High-Altitudes or SCATHA mission). Electron fluxes and spectra from a selected region of space were compared with the National Space Science Data Center (NSSDC) AE-4 time-averaged model and earlier SC-3 data. The radiation doses in silicon and the fluxes penetrating various shielding thicknesses of aluminum were calculated for the measured and model spectra.

2. Instrumentation

The SC-3 experiment measures electrons, protons and alpha particles using a solid state detector telescope surrounded by a scintillation counter anti-coincidence shield. Logic configurations among the telescope detectors and the energy range of analysis are selectable from an internal memory providing a large number of possible modes of operation. The standard preprogrammed modes used routinely include two energy ranges for electrons (47 to 299 keV and 260 to 4970 keV) and four proton ranges spanning 1.0 to 200 MeV. The instrument geometric factor of $3 \times 10^{-3} \text{ cm}^2/\text{sr}$ and its orientation on the spinning vehicle allowed accurate measurement of the high fluxes of electrons and their pitch angle distributions in the outer radiation belt. A more detailed description of the experiment is published elsewhere (Ref. 1).

The P78-2 spacecraft was launched on Jan. 30, 1979 and on Feb. 2, 1979 was boosted into its final orbit with apogee at 43192 km, perigee at 27417 km, a 7.9 degree inclination and a period of 23.597 hours, which is nearly earth synchronous. The spacecraft is spin stabilized with a spin period of about one minute. This orbit traverses the region of geomagnetic space from $L = 5.3$ to 8.0 where L defines a dipole-

like magnetic shell on which trapped charged particles execute their spiral, bounce and drift motions. At the magnetic equator, L is the distance of the shell from the magnetic polar axis (in units of earth radii).

3. Data

The electron fluxes and energy spectra were selected for analysis at $L = 5.5$. This region is sampled by the satellite twice each orbital revolution near perigee. From ten minute periods centered at the $L = 5.5$ time, 4.5 minutes of spin averaged data in each electron energy range were accumulated for 12 crossings of the L shell in the period June 9 to 14, 1980. Three of these spectra that illustrate the trend of spectral "hardening", or an increase in the flux with increasing energy, are shown in Figure 1 along with a long term time-averaged model spectrum labeled "NSSDC AE-4 Mean" (Ref. 2). The AE-4 electron environment model developed by the NSSDC for epoch 1967 is for solar maximum and therefore should be directly comparable to the 1980 SC-3 data. From Figure 1 it is evident that the electron spectra early in the period before the onset of the magnetic storm were softer and less intense than the AE-4 model for energies greater than 1 MeV. By June 13 the spectra were more intense than AE-4 at high energies and at 2210 UT on June 14, the last data currently available for the period, the flux intensity for energies greater than 2.6 MeV was the highest observed to that time in the SCATHA mission.

In Figure 2 the differential fluxes in selected SC-3 analyzer channels are plotted versus time for all of the $L = 5.5$ data in the June 9 to 14 period. At the top of the figure, the geomagnetic index D_{st} is plotted. The sharp decrease in D_{st} and slow recovery over the three following days clearly mark the magnetic storm. While the low energy channel fluxes ($E \leq 200 \text{ keV}$) vary by as much as a factor of five, no trend is evident during the period. At high energies, the trend becomes most pronounced with the fluxes increasing monotonically by an order of magnitude from June 11 to June 14 in the 3.39 - 3.79 MeV channel. The relatively long storm recovery period with several minor negative D_{st} excursions indicating continued magnetic activity may account for the large buildup of high energy fluxes.

4. Analysis

The penetration of aluminum shielding by electrons was calculated for the spectra in Figure 1 using a computer program which gives an excellent simulation of electron scattering and energy loss by analytic solution of a Fokker-Planck diffusion equation. This code, an adaptation of the AURORA program developed by Walt et al., (Ref. 3), treats the geometry of electrons with a specified angular distribution incident on a plane shield medium. The penetration depths of the fluxes obtained by integrating each of the four spectra above several energies with isotropic angular incidence on one side of a plane

Mappings of Energetic Electron Precipitation Following Substorms Using the Satellite Bremsstrahlung Technique

W. L. IMHOFF, J. STADSNES*, J. R. KILNER, D. W. DATLOWE,
G. H. NAKANO, J. B. REAGAN AND P. STAUNING†

Space Sciences Laboratory, Lockheed Palo Alto Research Laboratory, Palo Alto, California 94304

With an array of collimated cadmium telluride spectrometers on a spinning polar-orbiting satellite (P78-1) a study has been made of the energetic bremsstrahlung X ray ($> 21\text{-keV}$) patterns following substorms. From an altitude of ~ 600 km, X rays emanating from a wide range of magnetic local times can be observed and the local time profiles mapped on a given pass of the satellite across either polar cap. Pronounced longitude variations in the X ray intensities and hence in the precipitating electron fluxes were observed in the daytime sector at various delay times after the onset of substorms near local midnight. The longitude profile features were found to persist over time periods of at least a few minutes. Longitude variations in the energy spectra of the bremsstrahlung X rays were also obtained, and in several cases the spectra were found to be harder at later local times after midnight, although no consistent trends were evident. Coordinated measurements of electrons from the SCATHA satellite at near-synchronous orbit revealed enhancements in the fluxes of trapped electrons on the dayside at the times of the X ray events, indicating a correlation between the trapped and precipitating electron fluxes. Additional information on the longitude profiles of electron precipitation was obtained from riometer measurements in the Danish chain, which also provided complete time histories at the station longitudes. The longitude distributions of energetic electron precipitation as inferred from satellite X ray intensity and from riometer absorption measurements show very good agreement. The riometer absorption at the Narssarsuaq station with a value of 7.3, comparable to the SCATHA values, was found to be very similar in time profile to the trapped electron fluxes measured at SCATHA, showing a close association between the trapped and precipitating fluxes of electrons.

INTRODUCTION

It has been postulated that electron precipitation in the mid-to-late morning hours may be directly associated with the injection and acceleration processes that occur during magnetospheric substorms in the midnight sector. This association follows from a combination of the longitude drift of electrons in the geomagnetic field and their precipitation. In the past the phenomenon has been studied with bremsstrahlung X ray measurements taken from balloons, with riometer data, and with direct electron observations at synchronous altitude. From balloon X ray measurements, Barcus and Rosenberg [1966] found that very extensive and intense precipitation events are observed after dawn and that their occurrence is frequently correlated with a polar substorm. Using direct electron measurements at geosynchronous altitudes Pfister and Winckler [1969] postulated a model in which energetic electrons are created near local midnight and then gradient drift to later local times. Evidence for large-scale azimuthal drift of electrons during substorms was obtained by Arnولد and Chan [1969] and by Rosen and Winckler [1970] from comparisons of synchronous orbit data with ground-based riometer measurements. From simultaneous measurements in the equatorial plane and at balloon altitudes, Parks [1970] found that the flux versus time profiles between precipitated and trapped electrons are extremely well correlated at local times between midnight and noon. With ATS 5 data, DeForest and McIlwain [1971] discovered that a hot cloud of plasma is injected into the midnight sector of the magnetosphere during each substorm

and that subsequently energy- and pitch-angle-dependent dispersions occur.

Further experimental support for the drift hypothesis has come from the large-scale balloon observations of Sletten et al. [1971], who found that the average delay for onset of X ray events increases with increasing separation from the midnight sector. This was interpreted as an effect of the drift of electrons in the magnetosphere from an acceleration region on the night-side of the earth. Maral et al. [1973] discovered that the onsets of X ray events become steadily more gradual as one goes toward greater drift paths from the presumed acceleration region. Kangas et al. [1974, 1975] found that morning activity (often called SVA, slowly varying absorption, events) is delayed with respect to the midnight activity though the time delay varies from event to event. The energy spectral variations during the SVA events in which the X ray flux softens initially can generally be interpreted in terms of a drifting cloud of electrons. The riometer data of Berkey et al. [1974] indicate that the dayside precipitation 1–2 hours after substorm onset can be fairly localized (1–2 hours in longitude), with the local time for maximum precipitation shifting eastward to later MLTs at longer times from substorm onset. In most of these earlier studies the particle distributions were assumed to move only along a meridian or only in longitude, but it has been emphasized by Kivelson and Southwood [1975] that acceleration, inward motion, and east-west drift are strongly coupled processes in many instances.

In some SVA events, enhanced ionization occurs at altitudes below the normal scattering height for forward scatter HF and VHF transmissions, estimated to be ~ 75 km, and such events are then also classified as relativistic electron precipitation (REP) events since it is thought that precipitated electrons with energies between 0.1 and 1 Mev are principally responsible [Bailey, 1968; Rosenberg et al., 1972]. After onset of a substorm the delay time for daytime precipitation of energetic electrons

* Permanent address: Department of Physics, University of Bergen, Bergen, Norway

† Geophysical Department, Meteorological Institute, Copenhagen O, Denmark

Satellite Bremsstrahlung X Ray Measurements at the Onset of a Magnetospheric Substorm

W. L. IMHOFF, J. STADSNES¹, J. B. REAGAN, J. R. KILNER, E. E. GAINES, D. W. DATLOWE,
J. MOBILIA, AND G. H. NAKANO

Space Sciences Laboratory, Lockheed Palo Alto Research Laboratory, Palo Alto, California 94304

Bremsstrahlung X ray (>21-keV) mappings and direct electron (>68 keV) measurements from the low-altitude polar-orbiting satellite P78-1 were performed at critical times and locations near the onset of a magnetospheric substorm on July 3, 1979 at ~2149 UT. The bremsstrahlung X ray intensities emitted from the atmosphere over a wide range of longitudes and L shells were negligible just before the substorm onset, then rose to a maximum within about a minute or less, and remained at an enhanced level for the next 9 minutes. The onset time for the total intensities of X rays observed from the P78-1 satellite was nearly the same as for the X ray flux increase at one of the SBARMO-79 balloons which were at fortuitous positions during the event and within the field of view of the satellite X ray detectors. The simultaneous X ray measurements from the SBARMO-79 balloons and the P78-1 satellite indicate that the electron precipitation started at $L = 3-5.5$ without a significant precipitation from higher L shells. In addition, the satellite data revealed a relatively sharp longitude decrease in electron precipitation at positions east of ~30°E or at magnetic local times after ~1.5 hours.

INTRODUCTION

At the onset time of a substorm, energetic electrons are precipitated into the atmosphere, and the global spatial and temporal morphology of this precipitation should reflect the importance of local acceleration processes in comparison to azimuthal drift or propagation effects of particles accelerated elsewhere. Higher energy electrons (in the tens of keV region and upward) represent a significant portion of the electron energy associated with a substorm, and they can also provide important tracings of the magnetic field topology and an indication of the more energetic acceleration processes. The question of whether the energetic electrons come from an existing population or are freshly accelerated is a very important consideration that has been addressed by several authors. It was found by DeForest and McIlwain [1971] that clouds of hot plasma are injected on a one-to-one correspondence with magnetospheric substorms. The plasma injected at times of substorms will subsequently disperse in energy dependent clouds driven by the residual electric field and by the magnetic gradient and curvature drifts, as investigated by McIlwain [1974]. Moore *et al.* [1981] have considered substorm plasma injections in which boundary motion plays a major role. Based on the lack of riometer response at higher latitude stations in several events, Baker *et al.* [1981a] concluded that the injected electrons are newly accelerated. When detailed information on the spatial, temporal, and spectral characteristics of the precipitation become available, one might hope to learn more about the important question of whether a substorm is a directly driven process [Akasofu, 1979, 1980] or whether there is a growth phase [McPherron, 1970, 1972; Baker *et al.*, 1981a, b]. However, the spatial dynamics of energetic electron precipi-

tation at the onset time of a substorm has not been well studied partly because of the difficulties of obtaining continual worldwide mappings at those energies. Until remote sensing measurements of the precipitation of higher energy electrons are performed from high-altitude satellites, it will probably be necessary to piece the information together from available data covering more limited regions of space and time.

Proper studies of the precipitation of energetic electrons at the time of a substorm can best be made from widespread spatial and temporal observations. In this regard, riometer measurements have been restricted in spatial extent and direct particle observations from satellites or rockets are quite limited in their usefulness, although in certain cases simultaneous measurements from more than one vehicle have proven to be very useful [e.g., Rossberg, 1976; Rossberg *et al.*, 1977]. High-resolution spectral and pitch angle measurements near the equator at synchronous altitude [e.g., Parks *et al.*, 1977] have provided important information on the source locations of particles during substorm events. Postsubstorm electron precipitation extending through the daytime sector has been investigated with bremsstrahlung X ray measurements from low-altitude satellites [Imhof *et al.*, 1978, 1982] and from balloons [Barcus and Rosenberg, 1966; Sletten *et al.*, 1971; Maral *et al.*, 1973; Kangas *et al.*, 1974, 1975], but X ray mappings right at the onset time of a substorm are not generally available. Only a few X ray results during the initial phases of the auroral substorm, lasting 0-5 minutes [Akasofu, 1968], have been published [e.g., Bjordal *et al.*, 1971; Pytte and Trefall, 1972; Pytte *et al.*, 1976; Mauk *et al.*, 1981; Kremser *et al.*, 1982]. The lack of many observations may follow from the short time duration and narrow latitude extent. The onset phenomena are best studied with use of data from many widespread coordinated measurements, and for this purpose the satellite bremsstrahlung technique can be particularly useful. For example, worldwide mappings may enable one to identify strong longitude variations, such as the occurrence of growth in one longitude sector while expansion is going on in another, as suggested by Wiens and Rustoker [1975]. Also,

¹ Also with the Department of Physics, University of Bergen, Bergen, Norway.

Copyright 1982 by the American Geophysical Union.

Paper number 2A1087.
0148-0227/82/002A-1087\$05.00

REVIEW OF HOT PLASMA COMPOSITION NEAR GEOSYNCHRONOUS ALTITUDE

Richard G. Johnson
Lockheed Palo Alto Research Laboratory
and
University of Bern†

SUMMARY

The information available on the hot plasma composition at and near the geostationary satellite orbit has increased dramatically during the past four years. At energies below 32 keV, ions of terrestrial origin (O^+ and He^+) are frequently observed to be significant contributors to the hot plasma density and energy density, and during geomagnetically disturbed periods, O^+ ions are frequently the dominant ions. During geomagnetically quiet periods H^+ ions are typically the dominant hot plasma ions. Evidence for a solar cycle dependence to the O^+ hot plasma densities at the geostationary orbit has been found. Our understanding of the details of the physical processes involved in the entry, acceleration, transport, and loss of the plasma ions, and thus our ability to model them, is still quite limited.

INTRODUCTION

As recently as the 1st Spacecraft Charging Technology Conference in 1977, quantitative measurements on the ion composition of the hot (0.1-30 keV) plasmas near the geostationary satellite altitude had not yet been performed (ref. 1). The plasma composition in this region of the magnetosphere was inferred primarily from composition information obtained on similar magnetic L-shells but at much lower altitudes. Such observations led to the conclusion that, at least during geomagnetically disturbed periods, there were significant fluxes of O^+ ions as well as protons in the hot plasmas near the geostationary satellite altitude and that the ionosphere was the origin of the O^+ ions as well as some of the protons (ref. 1).

Prior to the work of Shelley et al. (ref. 2) in 1972, it was generally believed that the energetic ion population in the magnetosphere was always dominated by protons (H^+) and that the source of these ions was the solar wind (ref. 3 and 4). This viewpoint was specifically reflected in the summary of the

†Most of the unreferenced data presented in this review was reduced and analyzed while I was a Visiting Professor at the University of Bern. I am indebted to Professor J. Geiss and Dr. H. Balsiger for making the visit possible and wish to thank them and other members of the staff at the Physikalisches Institut for making my visit both productive and enjoyable. This research was sponsored by the University of Bern and the Lockheed Palo Alto Research Laboratory.

SCATHA OBSERVATIONS OF SPACE PLASMA COMPOSITION DURING A SPACECRAFT CHARGING EVENT†

R. G. Johnson, R. Strangeway, S. Kaye, R. Sharp, and E. Shelley
Lockheed Palo Alto Research Laboratory

SUMMARY

During the earth eclipse of the SCATHA spacecraft on 28 March 1979, the spacecraft charged to potentials greater than 1KV for about 30 minutes with extended excursions greater than 4KV. The composition of the hot plasma was obtained in the 0.1 to 32 keV energy range with an ion mass spectrometer aboard the spacecraft. Prior to the onset of the charging event, H^+ was the principal plasma ion, and during the event O^+ was the principal ion. The composition was energy dependent and varied significantly on a time scale of 4 minutes. An assumption that the ion flux was all H^+ would lead to computed number densities that were in error by more than a factor of 2 for several time intervals during the event.

INTRODUCTION

The number density of the hot plasmas that produces spacecraft charging is frequently determined from on-board measurements of the ion fluxes with energies above the spacecraft potential. To determine ion densities from flux measurements, mass composition of the plasmas must be known or assumed. Also, the secondary electron production by keV ions incident on spacecraft surfaces is often strongly dependent on the ion mass. Prior to 1977 when hot plasma composition measurements at high altitudes in the equatorial regions began, it was generally assumed that H^+ was the dominant hot plasma ion (ref. 1). Measurements extending up to 32 keV have now established that O^+ ions are frequently significant contributors to the plasma density and during times of high geomagnetic activity are often the dominant hot plasma ions (ref. 1, 2, 3).

The SCATHA spacecraft has provided the first opportunity near the geostationary spacecraft altitude to obtain the hot plasma composition during spacecraft charging events that produce potentials above a few hundred volts. (The GEOS spacecraft, which also obtained hot plasma composition measurements (ref. 2), did not charge to high potentials.) This report provides composition information during the charging event on 28 March 1979 with a time resolution of 4 minutes.

[†]This research has been sponsored by the Office of Naval Research and the U.S. Air Force under contract N00014-76-C-0444, and by the Lockheed Independent Research Program.

Hot Plasma Composition Results from the SCATHA Spacecraft

R. G. JOHNSON,* R. J. STRANGEWAY,* E. G. SHELLEY,*

J. M. QUINN,* and S. M. KAYE**

*Lockheed Palo Alto Research Laboratory, Palo Alto, California 94304, U.S.A.

**Plasma Physics Laboratory, Princeton University, Princeton, New Jersey 08544, U.S.A.

(Received July 19, 1982)

The SCATHA spacecraft provides hot plasma (0.1-32 keV) composition measurements near the equatorial plane in the L -shell range from about 5.3 to 8.3. The SCATHA mass spectrometer has provided the first routine pitch angle distribution measurements as a function of the ion mass near the equatorial plane and has doubled the upper energy range of previous plasma composition measurements. Ion pitch angle distributions are often found to be highly anisotropic, temporally/spatially structured, and mass dependent. During geomagnetic storms, hot plasma ions of ionospheric origin are found to be a major and frequently dominant component of the ion number and energy densities in the outer ring current region of the magnetosphere. Following magnetic substorm-injection events, energy-dispersed drifting ion clouds observed at the SCATHA orbit often contain large fluxes of O^+ ions and provide insight into the spatial/temporal history of the ions. The composition of the intense warm (about 10-500 eV) ion fluxes trapped within a few degrees of the magnetic equator has been found to be dominated by H^+ ions at the measured energies above 100 eV.

1. Introduction

The SCATHA spacecraft was launched in January 1979 into a high altitude elliptical and nearly equatorial orbit to investigate spacecraft charging at the high altitudes (hence SCATHA) and to investigate the plasma and wave environments which lead to spacecraft charging. A wide range of particle and field instrumentation was included in the payload, as well as ion and electron guns and a set of engineering experiments for spacecraft charging studies. Details on the instrumentation and on the program objectives are contained in a report by STEVENS and VAMPOLA (1978).

The SCATHA spacecraft is in a nearly geosynchronous orbit with apogee at $7.8 R_e$, perigee at $5.3 R_e$, and an inclination of 7.9° . The orbital period is 23.7 hours, resulting in an eastward drift of the groundtrack by about 5° per day. The spacecraft is spin stabilized with a spin period of one minute. The spin axis lies in the orbital plane and is perpendicular to the sun-earth line typically within 5° .

The SCATHA payload includes the Lockheed ion mass spectrometer for hot plasma composition measurements in the energy range 0.1 to 32 keV/q. The mass

The Radial Gradient of 0.1- to 32-keV H⁺ and O⁺ and the Azimuthal Wave Electric Field as Inferred From a Large-Scale Dayside Pulsation

S. M. KAYE¹ AND E. G. SHELLEY

Space Sciences Laboratory, Lockheed Palo Alto Research Laboratory, Palo Alto, California 94304

In this report we use 0.1- to 32-keV H⁺ and O⁺ flux modulations observed during a large-scale dayside pulsation event at $\sim 6 R_E$ near the equatorial plane on April 4, 1979, to estimate the azimuthal wave electric field and spatial radial gradient of the phase space densities for the two ion species as a function of energy. We first find that the average azimuthal electric field associated with the wave has an amplitude of approximately 10 mV/m; this electric field magnitude can cause field lines to be displaced $\sim 1.5 R_E$ during the course of an oscillation. Because of the large field displacement we can infer the ion distribution spatial radial gradients from a theoretical expression which describes the effects of a resonant hydromagnetic wave on a particle distribution. We find that for both H⁺ and O⁺, $\partial f / \partial R < 0$ for all energies. In addition, we find that the spatial scale length for changes in f for both O⁺ and H⁺ is generally of the order of several earth radii.

INTRODUCTION

In recent years the capability of using particle measurements to study hydromagnetic oscillations of the magnetosphere has been realized. Various studies have used observations of particle oscillations to analyze different features of the hydromagnetic wave. Lin *et al.* [1976] showed that local Fermi and betatron acceleration in compressional wave events with 2- to 12-min periods could account for the observed oscillations of 50-keV to 1-MeV electrons. From the 90° phase shift between the plasma and Pc 4 magnetic waves, Cummings *et al.* [1978] inferred that they were seeing standing field line oscillations with the plasma oscillations caused by the $E \times B$ drift motion induced by the wave electric field. Kokubun *et al.* [1977] arrived at a similar conclusion for low-energy (<600 eV) plasma oscillations during a Pc 5 event, but they also found that the phase of 79- to 330-keV particle oscillations with respect to the magnetic oscillation depended on energy and local time, suggesting a coupling between the magnetic drift motion of the energetic particles and the azimuthal electric field of the wave. Hughes *et al.* [1979] also found low-energy protons in quadrature with a compressional Pc 4 magnetic fluctuation, again indicative of the plasma drift velocity induced by the wave electric field, and they also found that the higher-energy protons were in antiphase with B and thus the total perpendicular pressure was conserved. Hughes *et al.* found further that electron oscillations at most energies were out of phase with B , and they concluded that the effects of the wave-induced drift velocity were not important because electrons have much higher thermal velocities than protons of the same energy. Singer and Kivelson [1979] used ion density fluctuations to identify the electric perturbation of a Pc 5 oscillation when Ogo 5 was at a node of the magnetic oscillation.

It is the purpose of this brief report to examine particle behavior during a large-scale, long-period compressional oscillation of the magnetosphere to infer properties of the wave as well as the spatial distribution of H⁺ and O⁺. The data that we will be using were obtained from the Lockheed ion mass spectrometer aboard the Scatba satellite. Scatba was launched into a near-equatorial, near-geosynchronous orbit in January

1979. Although similar in design to previous Lockheed instruments, the mass spectrometer aboard Scatba can sample the energy range from 0.1 to 32 keV/q. Previous instruments could measure the various ion species with energies only up to ~ 15 keV/q. The Scatba instrument is also capable of sampling practically the entire pitch angle range each spin (~ 1 min). For a more complete instrument description, see Kaye *et al.* [1981].

As we shall see, the large-scale and long-period wave event of interest prevents us from explaining the corresponding particle oscillations by a single mechanism. For instance, the betatron acceleration due to the compression of B cannot be used alone to explain the particle response; effects due to field line motion and the existence of a spatial radial gradient in the particle distribution as well as the acceleration of particles by the wave electric field must also be recognized. By assuming that the radial gradient of the particle phase space density, $\partial f / \partial R$, is independent of energy over a limited range of energies, we can estimate the azimuthal wave electric field from differences in the phase space density, at various wave phases, of ions in that energy range. Iterating this process, we find the best estimate for the wave electric field to be 10 mV/m $\pm 15\%$ peak to peak; such an electric field can cause a field line displacement of $\sim 1.5 R_E$.

With this value for the wave electric field we then compute the radial gradients ($\partial f / \partial R$) of H⁺ and O⁺ for energies from 1 to 32 keV. For the particular storm of interest, on April 4, 1979, we find that $\partial f / \partial R < 0$ for both H⁺ and O⁺ in the energy range from 1 to 32 keV. In addition, the spatial scale lengths for changes in f were typically of the order of several earth radii. We have previously shown (R. G. Johnson *et al.*, 1980) that during this storm, O⁺ was the dominant ion over the entire energy range. Furthermore, we presented evidence to suggest that the >1-keV O⁺ and H⁺ ions were energized in part by earthward adiabatic convection. The similarity of the radial gradients and spatial scale lengths for O⁺ and H⁺ that are calculated in this study is further evidence that for energies of >1 keV these two ion species underwent similar transport and/or acceleration processes.

OBSERVATIONS AND CALCULATIONS

The pulsation event of interest occurred on April 4, 1979, and was seen by instruments aboard Scatba from ~ 0400 to

¹ Now at Plasma Physics Laboratory, Princeton University, Princeton, New Jersey 08544.

Copyright © 1981 by the American Geophysical Union.

Observations of Transient H⁺ and O⁺ Bursts in the Equatorial Magnetosphere

S. M. KAYE,¹ R. G. JOHNSON, R. D. SHARP, AND E. G. SHELLEY

Space Sciences Laboratory, Lockheed Palo Alto Research Laboratory, Palo Alto, California 94304

Twenty-two days of data from the Lockheed ion mass spectrometer aboard the Scatna satellite were used to perform a statistical study of short-lived H⁺ and O⁺ bursts observed in the equatorial magnetosphere. The results of the study indicate that the ion bursts were transient phenomena occurring primarily in the nighttime sector during periods of enhanced geomagnetic activity. The average energy of the bursts, (W), was 1 keV, although the bursts were found to occur over any portion of the instrument's 100-eV to 32-keV energy range. Over one third of the observed bursts were associated with field-aligned electrons flowing from the same hemisphere as the bursts. The energy width ($\Delta W/(W) = 1$) and the pitch angle width (as great as 30°) of the bursts suggest that the ions had undergone substantial velocity space diffusion close to the geomagnetic equator.

INTRODUCTION

One of the more exciting topics in current space research is the role of the heavy ion constituent in magnetospheric dynamics. The picture that is emerging has the heavy ions acting as more than just a minor perturbation in the magnetosphere; as one example, Cornwall and Schulz [1979] and Kaye et al. [1979] demonstrated that both cold and energetic heavy ions could dramatically affect electromagnetic wave propagation below the H⁺ gyrofrequency and thus influence ring current decay. Heavy ions of ionospheric origin are not confined to the inner magnetosphere. Ghielmetti et al. [1979b], Frank et al. [1977], and Hardy et al. [1977] all observed streaming O⁺ in the magnetotail out to distances of $\sim 23 R_E$, $35 R_E$, and $60 R_E$, respectively.

Ionospheric ions can be used also as probes of adiabatic and nonadiabatic acceleration mechanisms at low altitude. Ion beams, distributions with peak fluxes in the direction of the magnetic field line, are indicative of a parallel acceleration mechanism and were frequently observed aboard S3-3 [Shelley et al., 1976; Sharp et al., 1977; Mizera and Fennell, 1977; D. J. Gorney et al., unpublished manuscript, 1979]. Evidence for a transverse heating mechanism has been in the form of the ion conic, a distribution symmetric about the field line direction whose flux peaks at some oblique pitch angle [Sharp et al., 1977; Mizera et al., 1977; Klumpar, 1979; Ungstrup et al., 1979]. Transverse heating was also inferred from the 10°–20° width (FWHM) of field-aligned ion distributions [Ghielmetti et al., 1978, 1979a]. The theoretical work of Kindel and Kennel [1971] indicated that electrostatic ion cyclotron waves, which could produce such transverse heating, could be destabilized by electron drifts at an altitude of several thousand kilometers. Lysak et al. [1980] used this idea to study theoretically ion heating by electrostatic ion cyclotron turbulence. Perkins et al. [1976] showed that these waves could be destabilized also by ion beams. Very recently, Kinner et al. [1979] presented simultaneous low-altitude observations of electrostatic hydrogen cyclotron waves and upflowing energetic ions (H⁺ and O⁺) demonstrating, for the first time, the close relation between these ions and waves. Lennartsson [1980] has suggested that transverse ion heating and generation of ion cyclotron waves arise as a natural consequence of

the interaction between the hot auroral plasma and the geomagnetic field.

In a previous study, Ghielmetti et al. [1978] performed a statistical analysis of upflowing ion events (UFI), consisting of both beams and conics, observed in the energy range from 500 eV to 16 keV on the S3-3 satellite. The key results of this study were that the UFI coincided spatially with the Feldstein auroral oval, the occurrence frequency of UFI increased with increasing altitude (showing a sharp rise in frequency at 5000 km), and the UFI occurred predominantly in the dusk local time sector with very few events between midnight and dawn local times.

In a very recent study, D. J. Gorney et al. (unpublished manuscript, 1979) extended the Ghielmetti et al. study by distinguishing between beams and conics in the energy range 90 eV to 4 keV. This procedure enabled Gorney et al. to point out the differences in character of the two types of distributions. For instance, during quiet times ($K_p \leq 3$) the conics exhibited a broad local time distribution peaked near noon, while the beam local time distribution peaked in the pre-midnight sector. Whereas conics were observed most frequently at altitudes greater than ~ 2000 km, beams were observed most frequently above 4000–5000 km. In addition, both the beams and the conics were found to occur more frequently at energies of <400 eV than at energies of >400 eV.

The situation changed during periods of high geomagnetic activity ($K_p \geq 3$). During these times, conical distributions were spread uniformly in local time, but beams exhibited a strong local time dependence with their occurrence probability peaking near dusk. The altitude distribution of beams remained unchanged, but the conics had an altitude distribution which increased systematically with altitude above 4000 km. Moreover, the beams were observed more frequently during disturbed than during quiet times, and during these disturbed times the beam energies were >2 keV approximately 50% of the time. In general, the results of the Gorney et al. study, which distinguished between beams and conics, were consistent with those of Ghielmetti et al., in which no distinction between the two types of distributions was made.

Downflowing ions on S3-3 were also reported by Ghielmetti et al. [1979a]. From the observed pitch angle widths (FWHM $\sim 20^\circ$) and from the fact that downflowing ion events occurred far less frequently than upflowing ion events, Ghielmetti et al. [1979a] concluded that strong pitch angle scattering was isotropizing the ion distributions in most cases within one half of a bounce period.

¹Present address: Plasma Physics Laboratory, Princeton University, P. O. Box 451, Princeton, New Jersey 08544.

Ion Composition of Zipper Events

S. M. KAYE, E. G. SHELLEY, R. D. SHARP, AND R. G. JOHNSON

Space Sciences Laboratory, Lockheed Palo Alto Research Laboratory, Palo Alto, California 94304

- A class of ion distributions has recently been identified by Fennell et al. (this issue). The distributions are composed of two components, a low-energy component with peak fluxes directed along the field line and a high-energy component with peak fluxes in the perpendicular direction. The transition between the two components occurs over a very narrow range of energies but can occur anywhere between approximately several hundred electron volts and 20 keV. Because of the appearance of this distribution on an energy versus time spectrogram, the ion events have been called zippers. The purpose of this report is to examine the mass composition of the zipper events. We find that the low-energy and parallel component is composed primarily of O⁺, with, to a lesser degree, H⁺ and a trace of He⁺. The high-energy and perpendicular component is predominantly H⁺, with the relative abundances of O⁺ and He⁺ down from those of the low-energy component by a factor of ~10. These results suggest that whereas the low-energy component is probably ionospheric in origin, the source of the high-energy component is most probably the plasmasheet.

INTRODUCTION

In a companion paper, Fennell et al. [this issue] present some rather interesting observations of ion distributions near synchronous altitudes. From data obtained aboard the SCATHA (P78-2) satellite, Fennell et al. found numerous examples in which the low-energy portion of the ion distribution peaked in a direction parallel to the field line, while the higher-energy fluxes peaked in a direction perpendicular to the field line. There was a well-defined transition energy anywhere between several hundred electron volts and ~20 keV at which the distributions changed from field aligned to trapped. When viewed in an energy versus time spectrogram format, the intermeshing of these two portions of the ion distribution within a narrow energy range gave the appearance of a zipper.

As is discussed by Fennell et al. [this issue], field aligned ion distributions in the equatorial region near synchronous orbit are not new. Field-aligned equatorial distributions have been reported by McIlwain [1975], Borg et al. [1978], Geiss et al. [1978], Comfort and Horwitz [1981], and Kaye et al. [1981]. The source of these distributions was generally believed to be the ionosphere. Fennell et al. attempted to determine whether the low-energy and parallel portion of their observed distributions originated from a source different from that of the high-energy and perpendicular portion. Although Fennell et al. suggested that indeed the two portions of the distributions had different sources, they deferred to the mass composition measurements to settle this question.

It is the purpose of this paper to investigate the ion mass composition of the zipper distributions observed by the SCATHA satellite to determine whether different source regions are implied for the high and low portions of the distributions. Such differences are in fact found. The low-energy and field-aligned portion of the zipper distribution is composed primarily of O⁺, along with some H⁺ and traces of He⁺, suggesting that this portion of the distribution was ionospheric in origin [Shelley et al., 1972; Johnson et al., 1974]. On the other hand, the higher-energy, perpendicular particles were primarily H⁺, with the relative O⁺ abundance down from that of the lower-energy population by about a factor of 10. Consequently, our results indicate that whereas the low-energy, parallel fluxes

were probably directly injected from the ionosphere, the higher-energy, perpendicular fluxes were most probably convected in from the plasmasheet.

The data that we use were obtained from the Lockheed ion mass spectrometer aboard the SCATHA satellite. The mass spectrometer is capable of measuring the various ion species in the energy range 0.1-32.0 keV and is capable of sampling practically the entire range of pitch angles each spin (~1 rpm). For a more complete description of the instrument, see Kaye et al. [1981], and for a description of the orbital parameters of the SCATHA satellite, see Kaye et al. [1981] or Fennell et al. [this issue].

For our study we examined eight zipper events, each event interval being 1 hour long. A list of the eight events, the satellite position midway through the interval, and the transition energy as identified on the Aerospace spectrograms (D. Croley, private communication, 1980) is given in Table 1. A selection criterion for the events was that the transition energy remain constant throughout the 1-hour interval.

DATA

Energy Spectra

The zipper events identified in the Aerospace spectrograms clearly showed a predominance of 90° pitch angle particles above the zipper energy and a predominance of 0° pitch angle particles below the transition energy. What will become clear

TABLE 1. Date, Universal Time, L Value, Dipole Latitude, Magnetic Local Time, and Transition Energy (as Identified From the Aerospace Spectrograms) for the Eight Zipper Events Studied Here

Date, 1979	UT	L	λ_\odot	MLT	Zipper Energy, keV
Feb. 22	1100-1200	7.7	8.1	6.5	~6
	2100-2200	6.7	15.9	14.3	2-4
March 28	0230-0330	7.5	-5.5	7.8	~10
	0400-0500	7.0	-3.6	9.0	~6
	0630-0730	6.4	-1.3	11.2	~4
March 29	0230-0330	7.4	-5.3	8.0	~10
March 30	0700-0800	5.5	-8.1	16.3	-3
April 4	0600-0700	5.8	-4.3	13.4	~4

Copyright © 1981 by the American Geophysical Union.

Composition Measurements of Warm Equatorially Trapped Ions Near Geosynchronous Orbit

J. M. Quinn and R. G. Johnson

Lockheed Palo Alto Research Laboratory, Palo Alto, CA 94304

Abstract. The mass composition of the intense warm ($E \sim 10\text{-}500$ eV) ion populations trapped within a few degrees of the geomagnetic equator in the range $L = 5.3\text{-}6.5$ are examined using data from the Lockheed Ion Mass Spectrometer on the SCATHA spacecraft. The equatorially trapped ions, within the measured energy range $E/q \geq 100$ eV, are found to be predominantly protons. These ions can be removed and replenished from the region sampled on time scales shorter than one day. Several recent works have focused on the energization of He^+ in the equatorial region by ion cyclotron waves. It is now evident that an energization and/or transport process is required which produces equatorial H^+ populations similar to those that have been predicted for He^+ .

Intense fluxes of ions trapped within a few degrees latitude of the magnetic equator in the range $L = 5.3 - 6.5$ have been reported by Olsen (1981) using data from the UCSD Charged Particles Experiment on the SCATHA spacecraft. These ions are extremely anisotropic with a peak at 90° pitch angle and decreasing by over an order of magnitude $10^\circ\text{-}20^\circ$ away from the perpendicular to the field line, with broader distributions at lower energies. The occurrence frequency for this population in the measured local time region from 0900-2200 was 30-50%. A systematic study of the composition of this population has not previously been conducted.

Recently several workers have focused on the possibility of a substantial He^+ population trapped in the geosynchronous equatorial region. Young et al. (1981) have reported GEOS -1 and -2 measurements showing He^+ heating to hundreds of eV coincident with the onset of ion cyclotron waves. Mauk et al. (1981) have interpreted a wave frequency gap near the He^+ cyclotron frequency as being due, in part, to He^+ ion cyclotron resonance. Mauk (1982) has also predicted that the wave generation process will leave an energized He^+ population concentrated predominantly near the geomagnetic equator ($\lambda < 3^\circ$). One candidate for wave-heated He^+ is the equatorially trapped ion population reported by Olsen (1981).

Morwitz et al. (1981) have examined "pancake distributions" below 100 eV using data from ISEE-1. These pancake distributions were found in both H^+ and He^+ . However the distributions observed by Morwitz et al. extended to magnetic latitudes of 30° (corresponding to an equatorial pitch angles of 34° in a dipole field) and included a broader selection criteria than the narrowly confined "equatorially trapped" population reported by Olsen. The observations of He^+ heating by Young et al. (1981) were more than 10° off the magnetic equator in three of the four cases investigated.

Copyright 1982 by the American Geophysical Union.

Paper number 2L0939.
0094-8276/82/002L-0939\$3.00

In the one case at 3.1° magnetic latitude, pitch angle data were not presented. Thus, their ion observations appear to be generally associated with a different population than that reported within a few degrees of the equator by Olsen (1981).

In this report we discuss results from the Lockheed Ion Mass Spectrometer onboard the SCATHA spacecraft for eight crossings of the magnetic equator during which the intense trapped ions with energies above 100 eV were present within a few degrees of the magnetic equator. Data from 3 of the 8 cases are presented and discussed in detail. The observations presented below show that the portion of the anisotropic, equatorially trapped, ion population above 100 eV/q consists primarily of protons.

The instrument consists of three analyzers, each covering 8 energy steps in contiguous portions of the range from 100 eV/q to 32 keV/q. The data in this report are taken from the "sweep" mode, in which each analyzer head cycles through 8 energy steps in 16 seconds, spending 2s at each energy. A 32 point mass-per-charge spectrum is sampled during each two second period. The FWHM pitch angle resolution is 5° . Pitch angle sampling is accomplished by spacecraft spin, with a spin period of approximately 1 minute. A more detailed description of the instrument is given by Kaye et al. (1981).

Observations

Three examples of equatorially trapped ions were chosen for detailed presentation. The energy range of the equatorially trapped population for the selected events extended well into the hundreds of eV, within the range of the mass spectrometer. The March 22, 1979 case may hold special interest because of its coincidence with one of the CDAW-6 periods. (The Sixth Coordinated Data Analysis Workshop (CDAW-6) is an international cooperative study focusing on energy transfer in near-Earth space for two selected periods.)

May 16, Day 136, 1979

The first case analyzed, day 136 of 1979, was chosen to allow direct comparison with the data published by Olsen. The SCATHA spacecraft at the time of interest was crossing the geomagnetic equator near local dusk, at a radial distance of approximately $5.5 R_E$.

In order to examine the mass composition of the equatorial ions, the data were sorted into six 15° pitch angle bins, folded about 90° . The counts in the lowest three energy channels (100, 129, 165 eV/q) were summed over the half hour interval from 18:00 to 18:30 UT. The counts/sample were then plotted versus pitch angle for the four species H^+ , He^+ , O^+ .

Figure 1 shows the relative counts per sample (including background) for H^+ and He^+ . The data have been normalized by the maximum counts/sample

Observation of Ionospheric Source Cone Enhancements at the
Substorm Injection Boundary

J. M. Quinn

Lockheed Palo Alto Research Laboratory
Palo Alto, California 94304

R. G. Johnson

Office of Science and Technology Policy
Washington, D. C. 20506

ABSTRACT

A large number of time varying electron and ion features, such as those observed in energy-time spectrograms of data obtained near geosynchronous orbit, have been previously explained through the use of an injection boundary model. This model describes such features in terms of the dispersion signatures of fresh, hot plasma which is "injected" into an extended region tailward of an injection boundary at the time of substorm onset. Using data from the Lockheed ion composition instrument and the UCSD electron and ion analyzers on SCATHA, we present two events indicating that innermost edge of the injection region is an especially important location for the substorm input of ionospheric ions. The injection signatures are identified by comparison of electron and ion data with the dispersion features predicted by various electric and magnetic field models. In both events the ion composition data show intense, narrow energy, field-aligned O^+ fluxes on the limiting edge of the dispersing ions. This feature corresponds to ions which can be backtracked to localized positions in the

vicinity of the injection boundary at the onset time. We conclude that the injection boundary, which corresponds statistically to the equatorward edge of the auroral oval, is at times the location of direct ionospheric input into the trapped, energetic particle population.

INTRODUCTION

One of the most commonly observed ion populations in the vicinity of geosynchronous orbit is the field aligned distribution occurring, typically, at energies below a few tens of keV. This pitch angle distribution was termed a "source cone" by Mauk and McIlwain (1975), in contrast to the loss cone distribution seen at higher energies. Fennel et al. (1981) studied occurrences of the combined source and loss cone distributions, which they called a "zipper distribution" because of the appearance of the spin modulated data on a spectrogram, and noted that substorm injection events both increase the intensity of the source cone ions and change the upper energy cutoff.

Geiss et al. (1978), during special maneuvers of the GEOS spacecraft which allowed good pitch angle sampling, reported ion composition measurements of low energy field-aligned ions which were apparently of recent ionospheric origin. A larger data base of composition measurements with good pitch angle sampling was provided by the SCATHA spacecraft which allowed Kaye et al. (1981) to determine that the source cone portion of the zipper distribution is composed primarily of O^+ . It should be noted however that these measurements were made near solar maximum, and long term studies of near 90 degree fluxes with the GEOS spacecraft (Young, 1982) imply a strong variation in ionospheric input with solar cycle. Although the data taken at geosynchronous altitudes clearly indicate an ionospheric source for the source cone population, the pitch angle distributions measured near the equator are fairly broad (half width approximately 20°) and

RESULTS OF THE SCATHA ION COMPOSITION EXPERIMENT DURING THE TMS

J. M. Quinn and E. G. Shelley

Lockheed Palo Alto Research Laboratory
-Palo Alto, California, USA

ABSTRACT

Hot plasma composition measurements ($E/q=0.1 - 32 \text{ keV/e}$), made with the near equatorial SCATHA spacecraft at geocentric distances of $5.3-7.8 R_E$, provided the first routine pitch angle distributions of ion composition in the vicinity of geosynchronous orbit. Pronounced pitch angle and spectral differences between ion species, in addition to temporal variations within each species, are indicative of many of the complex source, energization, transport, and loss mechanisms at play in the magnetosphere. Ion populations of interest include: 1) field aligned ions below several keV which are primarily ionospheric; and 2) more energetic ions peaked at 90° pitch angle, and 3) intense equatorially trapped ions below a few hundred eV, which are composed primarily of protons. Ionospheric plasma has been observed to take part in the substorm injection process, and there is evidence of an enhanced ionospheric source at the inner edge of the injection region.

Keywords: Ion Composition, Ionospheric Ions, Substorm Injection, Equatorially Trapped Ions, Pitch Angle Distributions, Source Cone Ions

1. INTRODUCTION

The SCATHA spacecraft (P7A-2) was placed into an elliptical orbit with apogee of $7.8 R_E$ and perigee of $5.3 R_E$ in February, 1979. The orbit inclination is approximately 8° and the period is somewhat less than 24 hours, resulting in an eastward drift of the groundtrack of $\sim 5^\circ/\text{day}$. The spacecraft spin period is nearly one minute, with the spin axis lying in the orbital plane, perpendicular to the earth-sum line.

The Lockheed mass spectrometer on SCATHA makes composition measurements of ions in the energy range $E/q = 0.1 - 32 \text{ keV/e}$ and the mass range $M/q = 1-32 \text{ AMU/e}$. The instrument is oriented 11° from the spin axis normal and routinely obtains good pitch angle coverage, with the look direction often passing within a few degrees of parallel or anti-parallel to the magnetic field. Pitch angle resolution is 5° FWHM. Further details of this and

other SCATHA instruments are given by Stevens and Vampola (Ref. 1). A recent review of the SCATHA hot plasma composition results is given in Ref. 2.

2. SOURCE CONE IONS

Two frequently observed ion populations seen near geosynchronous orbit are the field-aligned ions at energies below several keV (termed the "source cone" by Mauk and McIlwain, Ref. 3) and the loss cone distribution at higher energies. The combination of these two populations was called a zipper distribution by Fennel et al. (Ref. 4) because of its appearance in an energy-time spectrogram. The composition of these distributions was studied by Kaye et al. (Ref. 5) who found that the low energy, field-aligned population is dominated by O^+ and that the higher energy distribution, peaked at 90° , is composed primarily of H^+ . They concluded that the source cone population is most likely ionospheric in origin and that the high energy component is from the plasma sheet.

Figure 1 illustrates some typical composition and pitch angle signatures seen near geosynchronous orbit. The figure contains energy-time spectrograms, with inverted energy scales, for H^+ in the top panel and O^+ below. In order to indicate pitch angle dependences in a single figure, the data have been sorted into bins for "field-aligned" ($0^\circ \pm 30^\circ$ and $180^\circ \pm 30^\circ$) and "perpendicular" ($90^\circ \pm 30^\circ$). For each half hour interval, the data from these two bins are plotted adjacent to each other. The interpolated image thus resembles a spin modulated spectrogram, with the square wave between the H^+ and O^+ data panels indicating the plotting positions of the two pitch angle bins. The source cone ions, dominated by O^+ , are clearly seen in Figure 1, covering a broad energy range below several keV, from about 6:00-11:00 UT and following 14:00 UT. High energy H^+ fluxes, peaked at 90° , are apparent throughout most of the day. In addition to the fairly stable source cone distributions, field aligned transient bursts of O^+ and H^+ ions have been observed (Ref. 6).

3. IONOSPHERIC INPUT NEAR THE SUBSTORM INJECTION BOUNDARY

The enhancement of the field aligned ionospheric component in conjunction with substorms was studied

To be published in
Proceedings of the Symposium on the
'Achievements of the IMS'
1984

Outer Zone Energetic Electron Spectral Measurements

J. B. Reagan,* R. W. Nightingale,† E. E. Gaines,‡ and W. L. Imhoff§

Lockheed Palo Alto Research Laboratory, Palo Alto, Calif.

and

E. G. Stassinopoulos¶

National Space Science Data Center, Greenbelt, Md.

Detailed spectral measurements of energetic electrons between 47 and 5100 keV have been made with the SC-3 experiment aboard the P78-2 (SCATHA) spacecraft. During the period Jan. 29-Feb. 2, 1979 the spacecraft was in a highly elliptical orbit. Measurements of the outer radiation belt electrons from 3.5 to 8.0 Earth radii were made near the geomagnetic equator. Spin-averaged electron spectra in 12-24 energy channels have been obtained. The magnetic activity at the time of the measurements was low, but a modest magnetic storm ($D_s = -79$ nT) had occurred ~10 days earlier. Comparisons of the measured radial profiles and electron spectra with the NASA AE-4 and AEI-7 HI/LO radiation models have been made. Under these conditions the measured data are in better agreement with the AE-4 model than with the AEI-7 HI model, although the present data are more intense above 4 MeV than the AE-4 model. The impact of the measured spectrum on the dose profile encountered by a synchronous orbit satellite has been examined. For thin aluminum shields (<0.45 cm) the dose received is comparable using either the AE-4 or AEI-7 models or the measured spectra. For thicker shields the bremsstrahlung dose dominates over the direct electron effects.

Introduction

THE USAF Space Test Program P78-2 spacecraft, known as the Spacecraft-Charging-At-High-Altitudes (SCATHA) mission, was launched on Jan. 30, 1979 into a highly elliptical transfer orbit having an apogee of 43,183 km, a perigee of 176 km, and an inclination of 27.3 deg. The spacecraft remained in this orbit until Feb. 2, 1979, at which time an adjustment was initiated to provide the final, near-synchronous orbit at 7.9 deg inclination with apogee at 43,192 km, perigee at 27,517 km, and period of 23.597 hours. Included in the P78-2 payload complement is a high-energy particle spectrometer known as SC-3. This spectrometer, which is described in detail in the mission description report,¹ measures energetic electrons between 47 keV and 5100 keV, protons between 1 and 200 MeV, and alpha particles between 6 and 60 MeV in several selectable modes of operation.

The P78-2 transfer orbit provided a unique opportunity to study the entire outer radiation belt region from 3.5 to 8.0 Earth radii distance near the geomagnetic equator during this solar maximum epoch. In particular, the fine resolution and extended energy range of the spectrometer provides the opportunity to define the spectrum of the energetic electrons for comparison with existing radiation belt models. These data are of significant interest to spacecraft designers and mission planners in that the electrons in the MeV energy range contribute the dominant radiation dose to satellites operating in this region of space.² Long-duration synchronous satellite missions are significantly constrained by the shielding that must be included to mitigate the degradation and damaging effects of these electrons and their associated bremsstrahlung. The optimum shielding design of such spacecraft is critically linked to the accuracy to which the very energetic electron fluence is known over the mission lifetime. Because of the short duration of the transfer orbit, the present data cannot

provide the long-term averages required for mission planning but can provide a complete radial profile of spectral shape and flux for comparison with the radiation models at this time in the solar cycle. In the final orbit the opportunity exists to analyze an almost continuous data base in the year 1979, and hopefully thereafter, between 3.2 and 8.0 Earth radii, which encompasses the synchronous orbit. When analyzed, these data should provide the long-term averages necessary for high-altitude spacecraft mission planning. In this first publication of the SC-3 results we confine our analysis to the transfer orbit period.

Experiment Description and Operations

In the transfer orbit the SC-3 experiment was operated during real-time acquisition intervals only since the satellite tape recorder was not yet operational. The satellite was also spinning at a high rate of 1.04 rev/s as compared to the final orbit spin rate of 1.0 rev/min. The spin axis of the satellite is maintained perpendicular to the sun-Earth line such that in a single spin the SC-3 instrument scans through a complete pitch angle distribution. Since the sampling rate of the SC-3 spectra is twice per second, integration over one-half of the spin period or 180 deg in pitch angle resulted, while in the final orbit pitch angle measurements every 3 deg are being routinely obtained. Because of the limited angular resolution and the lack of magnetometer data, only spin-averaged electron data are reported in this paper. The SC-3 experiment was operated primarily in the electron modes during this period although some limited proton data were acquired. When the spectrometer is powered on, automatic operation is achieved in a hardwired mode, called BACKUP, that measured electrons between 240 and 5078 keV in 12 quasilogarithmic energy channels. The spectrometer can also be operated from an internal memory which determines the sensor to be analyzed, the logic configuration between the several sensors in the solid-state particle telescope, and the energy range to be analyzed. The telescope, shown in cross section in Fig. 1, consists of a 200- μ -thick surface-barrier silicon detector, D, that is used to analyze electrons in the 47-300 keV energy range. Following this detector is a stack of five 2-mm-thick surface-barrier silicon detectors connected in parallel for a total stopping range of 1 cm. This detector stack, E, is used to analyze electrons between 300 and 5100 keV.

*Presented as Paper 80-0390 at the AIAA 18th Aerospace Sciences Meeting, Pasadena, Calif., Jan. 14-16, 1980; submitted Feb. 7, 1980; revision received Aug. 26, 1980. Copyright © American Institute of Aeronautics and Astronautics, Inc., 1980. All rights reserved.

†Manager, Space Sciences Laboratory.

‡Senior Scientist, Space Sciences Laboratory.

§Research Scientist, Space Sciences Laboratory.

¶Technical Development Leader, Space Sciences Laboratory.

¶Astrophysicist.

ROLE OF ENERGETIC PARTICLES IN CHARGING/DISCHARGING OF SPACECRAFT DIELECTRICS*

J. B. Reagan, R. W. Nightingale, E. E. Gaines,
R. E. Meyerott, and W. L. Imhof
Lockheed Palo Alto Research Laboratory

SUMMARY

The role that energetic particles in the substorm plasma have on the charging and discharging of typical dielectric layers used on spacecraft has been investigated using spectra and pitch angle distributions measured in situ on the SCATHA spacecraft prior to and during a few kilovolt differential charging event in eclipse conditions on 28 March 1979. The particle spectra have been input to deposition codes that determine the dose rate as a function of depth in kapton and teflon layers used in the SSPM experiment on SCATHA. The calculated ambient dose rates of a few rads/sec throughout the bulk of the sample are sufficiently high that radiation damage levels can be reached on the time scale of 1 year. Surface dose is a factor of 100 higher. Bulk conductivity profiles have been obtained from the dose rates using empirical relationships available in the literature. The radiation-induced bulk conductivities calculated at the peak charging time are found to be smaller than the intrinsic dark conductivity range of solar-conditioned kapton but higher than the corresponding value for teflon. The radiation-induced surface conductivities in both materials are significantly higher than their intrinsic values. It is concluded that in this event the surface potentials of both materials were determined primarily by the current density carried by the electrons in the energy range < 30 keV and that radiation-induced bulk conductivity changes were not important for kapton but may be for teflon. It is further concluded that surface charging occurred when the spectrum hardened and a corresponding larger fraction of the charging current density was carried by higher energy electrons. The measured charging spectrum in this event is within a factor of 5 of the maximum allowable trapping limit according to experimental verifications of the Kennel-Petschek theory. It is proposed that the charging current density at this limit, in conjunction with material properties, will directly determine the maximum possible surface potential in eclipse conditions. Based on the measured potential across the SSPM kapton sample in this event, the maximum likely surface potential to be encountered in a substorm having similar spectral characteristics has been estimated.

INTRODUCTION

The purpose of this paper is to assess the role that the energetic portion of the substorm plasma has on the charging/discharging of spacecraft dielectric materials such as kapton and teflon. It is a well established fact that the most severe charging of spacecraft operating at high altitudes occurs in the magnetic midnight-to-dawn time sector where substorms are highly prevalent and

* Work performed under ONR contract N00014-76-C-0444.

J. B. Reagan, R. W. Nightingale, E. E. Gaines,
R. E. Meyerott, and W. L. Imhof, "Role of Ener-
getic Particles in Charging/Discharging of Space-
craft Dielectrics," Spacecraft Charging Technology,
1980, NASA CP-2182, AFGL-TR-81-0270, pp. 74-85,
1981.

SPACE CHARGING CURRENTS AND THEIR EFFECTS ON SPACECRAFT SYSTEMS

J. B. Reagan, R. E. Meyerott, E. E. Gaines,
R. W. Nightingale, P. C. Filbert, and W. L. Imhof

Space Sciences Laboratory
Lockheed Palo Alto Research Laboratory
Palo Alto, CA

ABSTRACT

The range and limits on the space charging electron currents available in the near-geosynchronous orbit have been identified from a large SCATHA satellite data base. The most intense current densities observed were 0.8 nA/cm^2 at 1 keV and 0.5 pA/cm^2 at 1 MeV. The effects of these currents on both surface and internal charging of dielectrics have been modeled. In exposed dielectrics radiation-induced effects significantly increase the conductivity within the first few μm of the surface, produce permanent radiation damage, and affect the final potential of the sample. The calculated electric field profiles and surface potential of a $127 \mu\text{m}$ Kapton® sample are found to be consistent with the voltage measured aboard the SCATHA satellite during a charging event. The calculated field strength of $2 \times 10^5 \text{ V/cm}$ is below the spontaneous breakdown level. Transient electrical pulses observed in association with the charging may therefore be due to capacitive coupling effects rather than to breakdown. The electric fields and voltage internal to both plane-parallel and coaxial geometries containing a Teflon® dielectric enclosed between two conductors have also been modeled. Electric field strengths of a few $\times 10^5 \text{ V/cm}$ and internal potentials of several kV are calculated for these typical configurations when exposed to the direct electrons in unusually energetic events. These field strengths are near minimum breakdown level but the transient pulses observed on SCATHA may be associated with the internal redistribution of these high fields at the times of large and rapid flux changes or at the times that heavy cosmic-ray tracks locally discharge the highly charged dielectric.

INTRODUCTION

It is now well established that high-altitude spacecraft can at times experience charging in the space plasma. The key elements in the charging process are the intensity and the energy spectrum of the space plasma electrons. When the current carried by the incoming magnetospheric electrons that reach a spacecraft surface exceeds the current leaving that surface through photoemission, secondary emission, backscattering, and the incoming magnetospheric proton current, the surface must charge negatively to repel a portion of the incoming electrons until a current balance condition is

reached. Under sunlight conditions the incident electron current must exceed the relatively large photo-electron currents (typically a few nA/cm^2) that are leaving the surface before any significant charging will occur. Thus, daylight charging of spacecraft has been limited to the few 100 V range based on the maximum available space charging currents in the several to few 10 keV energy region. The charging currents in space are limited by magnetospheric wave-particle-interaction processes that force the precipitation of the electrons into the atmosphere when the limiting flux levels are exceeded [1].

THE IONOSPHERIC CONTRIBUTION TO THE PLASMA ENVIRONMENT IN NEAR-EARTH SPACE

R. D. Sharp and W. Lennartsson
Department 91-20, Building 255
Lockheed Palo Alto Research Laboratory
Palo Alto, California 94304

R. J. Strangeway
Institute of Geophysics and Planetary Physics
University of California
Los Angeles, California 90024

Submitted to Radios Science, 1984

ABSTRACT

Many C³I systems rely on satellites in geostationary and other near-earth orbits that are largely within the earth's magnetosphere. It has only recently been observed that the ionosphere plays a major role in determining the hot plasma environment in which these satellites must operate. Spacecraft charging, radiation effects, and degradation of sensitive surfaces used in optical and thermal control systems are attributable to the interaction of spacecraft with this ambient hot plasma, and these effects are especially serious for the newer satellite systems designed to function in orbit for a decade or longer. Recent energetic ion mass spectrometer observations have shown that the hot magnetospheric plasma in the energy range from about 100 eV to about 30 keV contains a large and variable O⁺ fraction which is essentially all of ionospheric origin. The other principal constituent is H⁺ which can be either of ionospheric or solar wind origin. The O⁺/H⁺ ratio of the plasma is an important parameter in modelling the spacecraft-plasma interactions to attempt to predict the magnitude of the above described effects. This report reviews the mass spectrometer observations by the International Sun Earth Explorer (ISEE-1) and the Spacecraft Charging at High Altitudes (SCATHA) satellites and examines the data for various signatures of the plasma sources. The relative contributions of the ionosphere and the solar wind to the plasma density are estimated in the altitude range from about 25,000 to 70,000 km on the basis of the ion composition. It is found that the ionosphere is an important or dominant source during both quiet and storm time conditions.

CIRCULATION OF ENERGETIC IONS OF TERRESTRIAL ORIGIN IN THE MAGNETOSPHERE

E. G. Shelley

Space Sciences Laboratory, Lockheed Palo Alto Research Laboratory
3251 Hanover Street, Palo Alto, California 94304

ABSTRACT

Energetic ion composition measurements have now been performed from earth orbiting satellites for more than a decade. As early as 1972 we knew that energetic (keV) ions of terrestrial origin represented a non-negligible component of the storm time ring current. We have now assembled a significant body of knowledge concerning energetic ion composition throughout much of the earth's magnetosphere. We know that terrestrial ions are a common component of the hot equatorial magnetospheric plasma in the ring current and the plasma sheet out to $\leq 23 R_E$. During periods of enhanced geomagnetic activity this component may become dominant. There is also clear evidence that the terrestrial component (specifically O⁺) is strongly dependent on solar cycle. Terrestrial ion source, transport, and acceleration regions have been identified in the polar auroral region, over the polar caps, in the magnetospheric boundary layers, and within the magnetotail lobes and plasma sheet boundary layer. Combining our present knowledge of these various magnetospheric ion populations, it is concluded that the primary terrestrial ion circulation pattern associated with enhanced geomagnetic activity involves direct injection from the auroral ion acceleration region into the plasma sheet boundary layer and central plasma sheet. The observed terrestrial component of the magnetospheric boundary layer and magnetotail lobes are inadequate to provide the required influx. They may, however, contribute significantly to the maintenance of the plasma sheet terrestrial ion population, particularly during periods of reduced geomagnetic activity. It is further concluded, on the basis of the relative energy distributions of H⁺ and O⁺ in the plasma sheet, that O⁺ probably contributes significantly to the ring current population at energies inaccessible to present ion composition instrumentation (> 30 keV).

INTRODUCTION

The fact that ions of terrestrial origin might represent a non-negligible component of the hot magnetospheric plasma was first reported more than a decade ago /1/. These early hot plasma composition measurements were acquired from a low altitude polar orbiting satellite and were sensitive only to the precipitating component of the ion distributions. While precipitating heavy ions (O⁺), inferred to be of terrestrial origin, were unambiguously identified in association with both magnetic storms /2,3/ and substorms /4/, specific knowledge of source locations, acceleration processes, and circulation patterns were lacking.

A terrestrial ion outflow in the form of the polar wind was predicted /5/, and observed /6/, but this outflow suffered in two ways as the potential source of the observed precipitating energetic ions. First, this classical, polar wind differed in composition from the observed energetic ions. It was dominated by H⁺ and He while the energetic ions were dominated by H⁺ and O⁺. Second, the polar wind ion temperature was expected to be only of the order of eV; thus, the higher (several keV) temperature of the precipitating ions could not have been achieved through simple adiabatic heating of this source through the convection process. Additional acceleration or heating would be required. The first direct observation of energetic, terrestrial ion outflow was provided by the eccentric polar orbiting 63-3 satellite, which detected keV H⁺ and O⁺ ions flowing outward along auroral field lines /7/. Further adiabatic energization of ions injected into the plasma sheet at these energies could easily account for the energy of the ions observed to be precipitating at lower latitudes during magnetic storms.

Starting in the late 1970s several spacecraft (GEOS-1, GEOS-2, ISEE-1, SCATHA) carrying energetic ion mass spectrometers were launched into near equatorial orbits providing ion composition data from a few R_E (earth radii) to 23 R_E. Ions of terrestrial origin were found to be an important constituent of most hot plasma regimes within the magnetosphere, including the storm time ring current /8-11/, the quiet time ring current /12,13/, the plasma sheet boundary layer /14/ and the magnetotail lobes /15,16/. Terrestrial ions were also detected in the low latitude magnetospheric boundary layer /14,17/. Ion composition measurements from the highly eccentric high latitude PROGNOZ-7 spacecraft have shown that

Presented at the
Topical Meeting of COSPAR ISCD on the
Plasma Circulation in the Magnetosphere

To be published in
Advances in Space Research, 1984

Mass Composition of Substorm-Related Energetic Ion Dispersion Events

R. J. STRANGEWAY AND R. G. JOHNSON

Lockheed Palo Alto Research Laboratory, Palo Alto, California 94304

The Lockheed ion mass spectrometer flown onboard the SCATHA (P78-2) spacecraft is used to study the mass composition of two ion dispersion events. The energy-dispersed ions are observed over the full energy range of the instrument (0.1-32 keV/q) in the noon-dusk local time sector. On one of the days, March 22 (day 81) 1979, the dispersing ions are first observed following an isolated substorm. A long period of low magnetic activity is present prior to the substorm on this day, and a decrease in D_{st} is observed following the first observation of the dispersing ions. On the second day studied, June 7 (day 158), 1979, the correlation between ground magnetic activity and initial observation of dispersing ions is not so clear, since the dispersion follows a period of high magnetic activity. Both dispersion events follow a marked reduction in the preexisting near-geosynchronous plasma near the noon sector. The mass composition shows that although there are similarities in the dispersion for both protons and oxygen, there are also distinct differences. Both species show a definite dispersion ridge, but the protons also have additional fluxes at energies greater than the dispersion ridge energy. It is proposed that the composition changes are attributed to localized injection of ionospheric plasma in the dusk-midnight sector, with proton-rich plasma sheet ions convecting past the spacecraft from larger radial distances. By using the ability to scan in pitch angle, it is noted that there are both pitch angle and mass dependences to the arrival times of the dispersing ions. Protons at 30° pitch angles arrive at the spacecraft before oxygen ions at the same pitch angle.

1. INTRODUCTION

A well-known substorm-related signature at near geosynchronous altitudes in the equatorial magnetosphere is energetic particle injection. *DeForest and McIlwain* [1971] reported observations of dispersing 'plasma clouds' for energies <50 keV from particle measurements on the ATS 5 particle spacecraft. The times at which the plasma clouds were detected were well correlated with substorm activity on the ground. *McIlwain* [1972, 1974] attributed the plasma clouds to electric and magnetic field drifts bringing particles sunward from the nightside magnetosphere. The data were used to develop a convection electric field and magnetic field model, which was used to trace drifting particle trajectories backwards in time to a source location that was close to the *Mauk and McIlwain* [1974] injection boundary. The *Mauk and McIlwain* injection boundary was also determined by using ATS 5 data, the position of the boundary being given by the local time at which the low-energy (<100 eV) part of the dispersing plasma was first encountered.

Besides the experimental observations there is a large body of theoretical work concerning convection and drifts (see, for example, *Chen* [1970], *Stern* [1975], *Kivelson and Southwood* [1975], *Ejiri* [1978], and *Kaye and Kivelson* [1979]). *Akasofu* [1977] gives a review of experimental and theoretical studies of magnetospheric convection. Arising from these and other studies, one viewpoint is that the dispersing ions (and electrons) are a result of modifications to the magnetospheric convection system, producing a movement to lower altitude of plasma sheet particles. The *Mauk and McIlwain* injection boundary is often taken to mark the location of the injected particles at the time of substorm onset.

Moore et al. [1981] have investigated several substorm-related injections by using data from ATS 6 and SCATHA

(P78-2). From their analysis, they proposed that at the time of substorm onset an 'injection front' of energetic particles propagates earthward from the plasma sheet. The passage of the injection front over the spacecraft is marked by a near dispersionless increase in particle fluxes. The injection front is accompanied by a compression wave, and this wave has the tendency to steepen gradients in the plasma as the injection front propagates inward, resulting in a sharp inner boundary. *Moore et al.* conclude that the *Mauk and McIlwain* injection boundary 'is not the site of dynamic injections but does mark the approximate inner limit of substorm activity.' Their conclusion was supported by the fact that the injection fronts were observed tailward (that is at larger radial distance and later in local time) of the *Mauk and McIlwain* injection boundary.

Thus far, only two preliminary reports have been made on observations of the mass composition of ion dispersion events [*Balsiger et al.*, 1982; *Johnson et al.*, 1982]. In this paper we investigate mass dependent characteristics in two ion dispersion events as observed at the SCATHA orbit by using the Lockheed ion mass spectrometer. We shall show that the dispersion events are associated with substorm activity, and that, as is expected, the dispersing ions originated in the dusk-midnight sector near the time of substorm onset. Since the mass spectrometer can discriminate between protons and oxygen, we can begin to address the question of the source of the dispersing plasma. That the oxygen signature has differences from the proton signature may have implications on the model proposed by *Moore et al.* We show that a local injection of ionospheric plasma near the time of substorm onset can explain some of the signatures in the energetic ion spectra for different masses.

2. INSTRUMENTATION AND DATA ACQUISITION

The data presented in the next section were acquired by using the Lockheed ion mass spectrometer flown onboard the SCATHA (P78-2) spacecraft. A more detailed description of the instrument and orbital parameters is given by

Copyright 1983 by the American Geophysical Union.

Paper number 2A1856.
0168-0227/83/002A-1856\$05.00

ON THE INJECTION BOUNDARY MODEL AND DISPERSING ION SIGNATURES AT NEAR-GEOSYNCHRONOUS ALTITUDES

R. J. Strangeway and R. G. Johnson

Lockheed Palo Alto Research Laboratory, Palo Alto, California 94304

Abstract. A simple particle drift model is used to investigate the applicability of the injection boundary concept to the ion dispersion event observed on March 22 (day 81), 1979. The model consists of a dipole magnetic field with a uniform cross-tail electric field plus a corotation field. A full spectrum of particles from 100 eV to 32 keV is injected at the $K_p = 6-$ Mauk and McIlwain injection boundary at the time of substorm onset on this day (1100 UT). A new approach is presented for displaying the model-produced ion drift trajectories to make the large scale spatial characteristics of the evolving energy distributions easier to envision and to facilitate the comparison of the model results with experimental observations. The resultant prediction for the dispersion signature is compared with Scatia mass spectrometer measurements, and a 2.0 kV/ R_e cross-tail convection electric field is found to give a good fit to the observed dispersion signature. It is determined that for this particular event, injection only at that portion of the injection boundary close to 1800 local time is required to produce the dispersion curve.

Introduction

Much work has been carried out on magnetospheric plasma convection and the associated particle signatures. Chen [1970] and Cowley and Ashour-Abdalla [1976], amongst others, have calculated drift trajectories for ions in the earth's magnetosphere. From steady-state drift analyses such as these, proton nose events (Smith and Hoffman [1974]) have been explained as a consequence of drift trajectory morphology. On the other hand DeForest and McIlwain [1971] have reported observations of dispersing particle signatures at geosynchronous altitude associated with substorms. These signatures are usually considered to be associated with impulsive changes in the magnetosphere. As a consequence the substorm-related injection boundary model as first formulated by Mauk and McIlwain [1974] has frequently been used as a starting point when discussing dispersion signatures.

There is still some controversy concerning the nature and possible existence of the injection boundary. For example, Kaye and Kivelson [1979] have modeled substorm-related particle signatures using steady state convection boundaries in their initial conditions. These boundaries have a radial dependence as a function of energy, whereas the injection boundary implies a co-located source for all energies. Taking elements from both these models, Moore et al. [1981] argued that the injection boundary marks the innermost excursion of a substorm related shock front which is propagating from the plasma sheet to lower L-shells. Strangeway and Johnson [1983] have suggested, from mass composition data, that there may be enhanced ionospheric plasma injected into the magnetosphere near the injection boundary. Their conclusion is not definitive, in that mass dependent radial gradients in the plasma sheet may alone be responsible for the composition differences observed in the dispersing ion signatures. Nevertheless one may speculate that an inward propagating shock front will perturb the ionosphere, possibly through field-aligned currents, and so result in enhanced deposition of ionospheric plasma into the magnetosphere.

In this letter we present some initial results of an investigation into the usefulness of an injection boundary model for producing the ion energy-time dispersion signatures observed near geosynchronous altitudes. In addition, we present a new approach for displaying the model-produced ion drift trajectories which makes the large scale

spatial characteristics of the evolving ion energy distributions easier to envision and facilitates the comparison of the model results with energy-time spectrograms of the experimental data. The results from a simplified injection boundary model are compared with the ion dispersion event observed on 22 March (day 81) 1979. This event has been analyzed and discussed by Strangeway and Johnson [1983], but no detailed model comparisons were made. We have chosen to further analyze this event since 22 March 1979 is a day which has been the subject of a major research effort arising from the Sixth Coordinated Data Analysis Workshop (CDAW-6). The data presented in this letter were acquired from the Lockheed mass spectrometer flown on board the near geosynchronous Scatia spacecraft. The ion measurements cover the energy range from 0.1 to 32 keV in 24 energy steps, and only proton and oxygen data are discussed here. For a more detailed description of the mass spectrometer characteristics and of the Scatia spacecraft orbit ($L \approx 5.8$), see Kaye et al. [1981].

Dispersion Model

A very simple model for the drift path calculation has been employed. The basic formulae used have been given by Chen [1970] and Cowley and Ashour-Abdalla [1976]. To summarize, we use a dipole magnetic field model, with a uniform cross-tail electric field plus a corotation electric field. No corrections due to shielding or magnetic field distortion have been included. In the model calculations we trace drift paths forward in time for an ensemble of ions starting at 128 locations on the Mauk and McIlwain injection boundary for $K_p = 6-$. The boundary was truncated at 1800 and 2400 LT. This boundary was chosen since K_p was equal to 6- at 1055 UT on March 22, 1979 when a substorm occurred (Strangeway and Johnson [1983]). At each particular location the drift paths for 96 different energy particles are traced. The energies are equally spaced on a logarithmic scale from 100 eV to 32 keV, which is the energy range of the Scatia mass spectrometer. For the particular event under consideration we have calculated drift paths for 90° equatorial pitch angle particles. It should be noted that we have assumed an impulsive injection of particles at the boundary coincident with the substorm onset, and no additional particles are included in the model subsequent to this time.

Figure 1 shows the results of the drift path calculation with 2.0 kV/ R_e cross-tail convection field. There is a large amount of information shown in this figure. Firstly the figure consists of 16 panels, each of which contains a snap-shot of the particle positions at a particular time, the times are given in the upper right hand corner of each panel, starting at 1100 UT (near the time of substorm onset on March 22, 1979), until 1445 UT at 15 minute intervals. The convection field strength is given in the upper left hand corner of each panel. A nominal magnetopause location is given by the yellow curve to the left of each panel, with the half illuminated circle giving the location of the earth. The small cross-hair indicates the Scatia spacecraft location as determined from the ephemeris information for March 22 (day 81), 1979, projected into L and local time (LT). As the cross-hair encounters the drifting ions, the color changes, so that the spacecraft location is always given in complementary color as shown, for example, in the first panel, second row. In the same panel some small white dots are present on the lower energy edge (blue) of the drifting plasma cloud. These dots mark the location on the original injection boundary of the ions which are at the Scatia spacecraft location at this time. In addition, we also build up a pseudo-spectrogram in the box in the lower right-hand side of each panel. The color coding of the dispersion signature thus produced is not a flux level, but is only given for reference to the color

Copyright 1983 by the American Geophysical Union.

Paper number 3L0706.
0094-8270/83/003L-0706\$03.00

Energetic Ion Mass Composition as Observed at Near-Geosynchronous and Low Altitudes During the Storm Period of February 21 and 22, 1979

R. J. STRANGEWAY¹ AND R. G. JOHNSON²

Lockheed Palo Alto Research Laboratory, Palo Alto, California

Mass composition data acquired during the storm period of February 21 and 22, 1979, are presented and analyzed. The data were obtained from the near-geosynchronous SCATHA spacecraft and the polar-orbiting S3-3 spacecraft at altitudes below 8000 km. The data from both spacecraft show that significant amounts of ionospheric plasma were observed to be injected around the main phase of the two storms on February 21, 1979. At geosynchronous altitudes the increase in ionospheric plasma was found to be significant in both number density and energy density. Moreover, multiple dispersionlike signatures in the particle spectrograms were observed during the second storm, indicating that this plasma was recently injected into the magnetosphere. At lower altitudes the S3-3 data also showed significant enhancements of ionospheric plasma, as determined from number density data. It was found that the density enhancement in the plasma population moved to progressively lower L shells during the recovery phase of the storms. As it is unlikely that the plasma is injected at the point of observation, at least during the recovery phase, we consider drift effects to be responsible for this signature. We hence summarize some of the simpler convection theory, specifically addressing the dependence of the boundaries between drift regimes as a function of L shell. To do this, a steady state convection model has been employed, but we assume that this "steady state" only applies during the recovery phase of the storm. Since we consider shielding to be important only later in the recovery phase, it is further assumed that the cross-tail electric field is uniform. On comparing the data with the convection boundaries we find that we can usually choose a cross-tail electric field strength which models the particle signatures quite closely. The major feature present in the particle spectra is an energy-dependent minimum which, we presume, marks those ions that either have been lost or drift so slowly that they are not observed at the spacecraft. As a consequence of the comparison of the S3-3 particle signatures with the predicted convection boundaries, we find that the apparent movement to lower L shells of the density enhancement during the recovery phase is due to time of flight effects on a low-energy plasma population at these L shells (below $L = 4$). Time of flight also implies that these ions were in the morning local time sector at the time of the main phase of the storms. At the same time that these low-energy ions drifting eastward are observed, large numbers of ions convecting westward are also seen. This plasma population contains a large amount of ionospheric plasma. Furthermore, the ionospheric plasma as labeled by singly charged oxygen appears to have been injected over quite a large range in local time during the first storm. However, the proton signatures imply that most of the protons observed at the higher L shells were confined to the nightside sector during the main phase of the storm. While there are many similar features associated with the second storm in the S3-3 data, the oxygen ions display a signature consistent with injection only in the nightside magnetosphere. This is in agreement with the SCATHA observations where the particle spectra show multiple dispersion signatures.

1. INTRODUCTION

During times of high magnetic activity, significant changes are known to occur within the earth's magnetosphere. Specifically, the ring current particle population is known to be modified at these times as shown by the D_s index and by direct measurements of the energetic particle populations. It has been argued by Lyons and Williams [1980] that the increase in the ring current population at storm times can be explained by inward convection of the preexisting plasma population. Mass composition data, however [Johnson et al., 1977; Balsiger, 1981; Johnson, 1981; Lennarsson et al., 1981; Hultquist, 1982; Lundin et al., 1982a; Young et al., 1982], indicate that there is a change in the composition of the lower-energy (< 17 keV/q) ring current population during times of increased geomagnetic activity, and it has been deduced that there is an enhanced injection of ionospheric plasma into the mag-

nosphere during storm times. Presumably, the increase in the ring current signature as observed at the ground is due to both these processes occurring at the same time; that is, enhanced inward convection of the preexisting trapped population together with an overall increase in the particle population due to injection. Although the relative contribution of the two processes to the storm time ring current remains to be determined quantitatively, Johnson [1981] and Johnson et al. [1983] have argued that in some storms the ionospheric component will be an important contributor to the ring current energy density because of the buildup of the ionospheric component in the hot plasma population prior to the main ring current injection process.

Mass composition data are a useful indicator in assessing the relative significance of both processes. Unfortunately, most storm time mass composition data is restricted either to the lower-energy component of the ring current, typically less than 17 keV/q, or to energies of the order of 1 MeV [e.g., Spieldesk and Fritz, 1981a, b]. Nevertheless, much can be learned concerning the effects of injection and convection on the magnetospheric ion population using such data. Strange-way and Johnson [1983], for example, have investigated the mass composition of ion dispersion events as observed at the near-geosynchronous SCATHA spacecraft orbit. It was found that the dispersing ions showed features within the compo-

¹ Now at Institute of Geophysics and Planetary Physics, University of California, Los Angeles.

² Now at Office of Science and Technology Policy, Executive Office of the President, Washington, D. C.

Copyright 1984 by the American Geophysical Union.

Paper number 4A0918.
0148-0227/84/004A-0918\$05.00

END

FILMED

2-85

DTIC